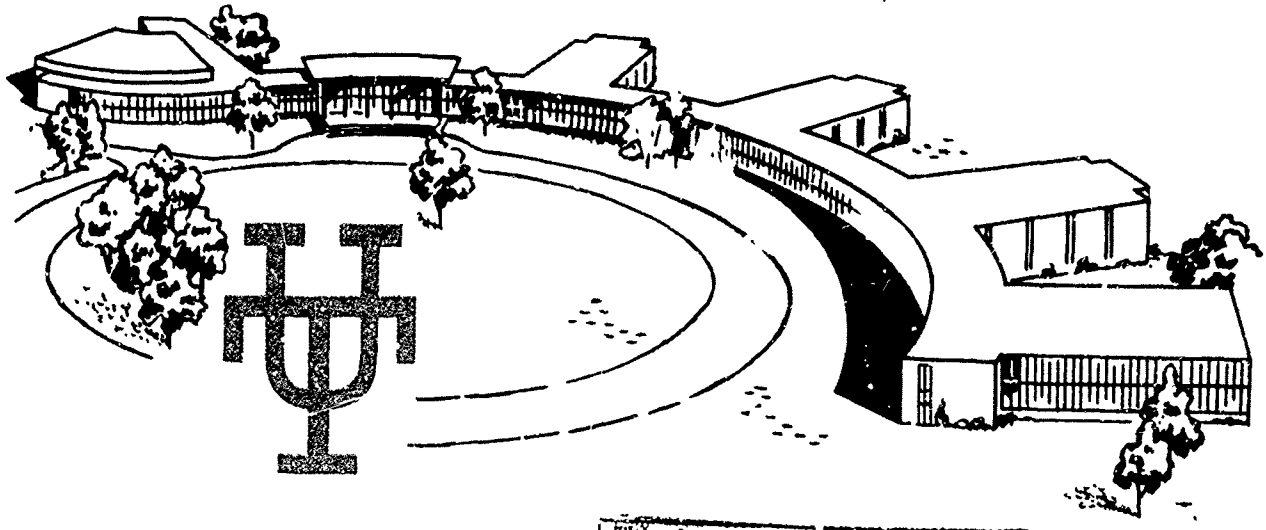

THE UNIVERSITY of TENNESSEE SPACE INSTITUTE

Tullahoma, Tennessee

DISCLAIMER NOTICE

THIS DOCUMENT IS BEST QUALITY PRACTICABLE. THE COPY FURNISHED TO DDC CONTAINED A SIGNIFICANT NUMBER OF PAGES WHICH DO NOT REPRODUCE LEGIBLY.

(2)

(6)

LASER VELOCIMETER MEASUREMENT OF THE CHRONOLOGICAL VELOCITY AT SELECTED POSITIONS IN THE MUZZLE BLAST FROM A 20-MM CANNON.

by

(10)
W. M. Farmer
K. E. Harwell
J. O. Hornkohl
R. Morris
F. A. Schwartz
L. Boyd
M. L. Kar

(12) 451

Gas Diagnostics Research Division
The University of Tennessee Space Institute
Tullahoma, Tennessee 37388

(9)
FINAL TECHNICAL REPORT
Contract No. DAAK40-77-C-0123
(11) September 1979
(5)

AD A111453

LASER VELOCIMETER MEASUREMENT OF THE CHRONOLOGICAL VELOCITY AT SELECTED POSITIONS IN THE MUZZLE BLAST FROM A 20-MM CANNON

W. M. Farmer, K. E. Harwell, J. O. Hornkohl, R. Morris
F. A. Schwartz, Larry Boyd, and M. L. Kar
Gas Diagnostics Research Division
The University of Tennessee Space Institute
Tullahoma, Tennessee

ABSTRACT

A real fringe laser velocimeter was used to obtain one dimensional chronological velocity measurements in the muzzle blast from a 20-mm cannon at selected centerline and barrel edge positions. Although data acquisition was slow allowing no more than 22 measurements per millisecond, the data show discernable flow features such as shock waves and mean flow velocities before and after passage of the projectile. The data clearly demonstrate the ability of real fringe laser velocimeter systems to obtain data in flow fields of this type.

1.0 INTRODUCTION

Chronological shadowgraph observations of the muzzle blast from a 20-mm cannon reveal a complex flow field with numerous shock and pressure waves which may be associated with the precursor flow and subsequent flow around the projectile. Because such flows are highly transitory with strongly refracting components such as shock waves and presumedly large numbers of particles, the probability of successfully using modern flow measurement techniques such as the laser velocimeter has been considered small at best. In an attempt to evaluate the capability of a laser velocimeter to obtain measurements in a muzzle blast, the UTSI Gas Diagnostics Research Division was tasked with attempting velocity measurements at selected points in the muzzle blast of a 20-mm cannon. The purpose of this report is to describe the results of those tests.

2.0 UTSI LV SYSTEM

The LV system used in these measurements may be conveniently divided into two major subsystems—1) optics and 2) electronics. This section describes these systems.

2.1 LV Optical System

The optical system used in these measurements was a real fringe type used in a near axis forward scatter mode. This mode of observation generally yields increased system sensitivity to small particles over that which could be obtained from backscatter. Figure 1 schematically shows the optical arrangement while Fig. 2 illustrates how the system was mounted with respect to the cannon. During operation the laser was operated at 400 milliwatts of power at a wavelength of 514.5 NM. A parallel surface beam splitter was used to produce two beams of nearly equal intensity. These beams were made to focus and cross to yield a fringe period of 28.5 micrometers and a probe volume diameter of about 400 micrometers. Light scattered by particles passing through the probe volume was collected with an F/6 aspheric telescope mounted approximately 9° off the bisector between the beams. An EMI 9781R photomultiplier tube (PMT) was used to detect the scattered light signal. Current generated by the PMT was amplified and transmitted to the UTSI Mobile laboratory which housed the signal processor and data acquisition system. Measurement and visual observation showed the probe volume depth of field to be approximately 5-mm.

2.2 LV Signal Processing and Data Acquisition System

Data acquired during a firing was recorded on magnetic disks after being transferred from the microprocessor memory. Any signal which was measurably periodic (aperiodicity $\pm$ 50% or less) over at least 12 signal cycles was recorded in memory. In this way the data could be interrogated for different levels of uncertainty in the measurements. This is accomplished by determining the average signal period for a preset number of cycles (in this case 12) and comparing this average with another of

different cyclic duration (in this case 7). If the averages agree within some acceptable tolerance (which may vary from ± 0.1 to ± 50% difference) the data point will be included in the ensemble of measurements. Generally as the tolerance increases so does the sample rate. Hence, a tradeoff in time resolution and measurement accuracy arises. For the measurements reported here the uncertainty in velocity was either 5 or 15%. As the data will show, the increase in temporal resolution is quite dramatic when the data are allowed to be uncertain by ± 15%.

Numerous reasons may be put forward as to why the LV signal might be aperiodic. Primarily, they reduce to multiple particles with different velocities in the probe volume or a particle accelerating across the probe volume. The latter is unlikely since for a tolerance of ± 15% a particle would have to experience accelerations greater than 10^7 m/sec^2 for mean speeds of 300 m/sec. to be rejected. Additional studies with the data for different values of tolerence in the data should prove interesting. However, such data has yet to be analyzed. Figures 3 and 4 schematically show the signal processing and data acquisition system and the measurement functions and data output options which are available with the entire electronics system. Because the signal frequency was beyond the frequency response of the particle sizing electronics only the velocity measuring portions were used. Maximum data acquisition rate possible with this system was approximately 22 measurements per millisecond. The transfer of data from the signal processor to computer memory being the limiting data rate factor. A method to increase the data acquisition rate to greater than 1000 per millisecond is discussed in the summary and conclusions section.

3.0 EXPERIMENTAL RESULTS

For convenience in operation and to facilitate additional experiments in Raman spectroscopy the cannon was mounted in a small test facility at AEDC. Ammunition for the cannon was provided by the Army and was specially loaded to about 1/2 typical charge strength. UTSI provided all signal processing and data acquisition equipment, and all optical components for the LV measurements except for an Ar^+ laser supplied by AEDC. These tests were

conducted from 1800-2200 hours on June 19, 20, and 21 1979. During this time approximately 56 rounds were fired. In this report, results for 16 different flow positions are given. At each position measurements were made for at least two firings. At 7 muzzle diameters down the centerline data were acquired from 4 consecutive firings to test data repeatability.

Initially several rounds were fired to optimize system performance. It was found that a significant portion of the data record was lost if the data sequence was triggered by the pressure transducers mounted near the end of the muzzle. With a minor trigger circuit modification, the data acquisition sequence was started at the same instant the round was fired. This sequence mode was used in nearly all the data reported here.

3.1 Transmissometer Measurements

It was found that projectile arrival at the probe volume varied slightly from shot to shot. In order to determine the projectile arrival time at the probe volume a powermeter was used as a photodetector for one of the transmitted LV beams (see Fig. 2). The output from the detector was photographically recorded from an oscilloscope trace which was triggered simultaneously with the data acquisition system. This arrangement also served as a crude transmissometer which was used to determine beam deflection or attenuation as a function of time. By observing the time position in the oscilloscope trace where the projectile passed through probe volume, reasonable definition of the precursor and after flow could be obtained. Figures 5 and 6 show the oscilloscope recordings of the transmissometer outputs for the centerline and barrel edge measurements. These recordings contain a number of interesting and distinctive features which may be associated with the muzzle blast. Observe, for example, the initial spike at X/D = 4 for the centerline measurements in Fig. 5. This spike is attributed to the gun muzzle flash. Since the laser power at the detector is 150 milliwatts, the spike shows that the flash must be quite bright. From these recordings we estimate a radiant intensity of about 1 kilowatt/ster. This assumes unit response of the photodetector for all wavelengths which is not the case. It should be anticipated that the radiant intensity will be less than

that quoted here. The passage position of the projectile is assumed to be those positions in the traces where the signal is completely blanked for about 0.2 milliseconds. The general trends in the transmissometer traces are in agreement with shadowgraph photos which show large areas of the flow to be dark either by flow refractions or large particle concentrations. An additional feature that shows up in these data is the sharp dip in transmission immediately after the muzzle flash spike. We believe this may be beam deflection due to a strong precursor shock wave. Figure 7 shows the transmissometer traces for 4 consecutive firings at X/D = 7. These data were taken in order to determine data repeatability. As Figure 7 shows, the general structure of the transmission remains the same from shot to shot. There is, however, roughly 0.5 to 1 millisecond of time variation between the firing trigger and the muzzle flash.

3.2 Velocity Measurements

The data acquisition system was set up to record up to 1000 velocity and relative time of occurrance measurements. The time of occurrence was read to the nearest microsecond. It was required that the Doppler signal have at least 15 cycles and satisfy an aperiodicity test of $\pm$ 50% before its time of occurrance and signal time period were entered into memory and later recorded on magnetic disk for permanent storage. After a typical shot the memory was interogated for a $\pm$ 15% uncertainty in the velocity for the preliminary evaluation of the data which is reported here.

The velocity data for the first 20 milliseconds beginning from the trigger event have been plotted as a function of time for the positions shown in Fig. 8. Figures 9 to 15 plot velocity as a function of time for measurements made on the centerline (Y/D = 0.0) of the projectiles path and the positions indicated in Fig. 8. Figures 16 to 22 plot velocity as a function of time for similar X/D positions and Y/D = -0.5. The approximate time of arrival as estimated from the transmissometer data is indicated as a straight vertical line on the plotted data.

A number of interesting features appear when these data are compared

for consecutive X/D values. Among the most obvious observations for measurements along Y/D = 0 are:

1. As X/D increases, the number of measurements occurring before the projectile reaches the probe volume is at first large, then decreases to practically zero, then increases again.
2. The dead-time in data acquisition after the bullet passes the probe volume is reduced to essentially zero after X/D = 2.
3. Until after X/D = 3, the precursor flow is definitely faster than the after flow.
4. The precursor and after flows are roughly the same after X/D = 6.
5. The highest precursor flow was observed at X/D = 1.
6. A surprisingly periodic precursor flow was observed for X/D = 3.
7. The highest mean value for the after flow is observed at X/D = 5.

General observations made for Y/D = -0.5 are

1. Relatively little precursor flow is observed for all X/D positions.
2. Precursor flow is generally at a higher speed than the after flow.
3. For X/D = 0, there is a long delay time before data acquisition begins.
4. As X/D increases most data appears immediately after the projectile passes the probe volume.
5. Very little of the after flow appears to be at sonic velocities.

Figures 23 to 26 plot velocity versus time for four consecutive shots made at X/D = 7, Y/D = -0.5 in order to determine data repeatability. General data trends are seen to be consistent, although exact data values are not constant as might well be expected. It is interesting to note that a very strong velocity component is consistently measured roughly 15 milliseconds after trigger.

The Gas Diagnostics Research Division at UTSI currently has under development a program to determine power spectral densities of flows as measured by an LV system. A number of different approaches have been attempted by previous investigators with some degree of success. The major problem in attempting such computations for an LV system is that the flow is sampled randomly. Previous algorithms have attempted to artifically manipulate the data to eliminate its random data acquisition characteristics in order to apply FFT (Fast Fourier Transform) algorithms to the power spectrum com-

putation. In so doing aliasing errors are introduced and it is usually required that the LV sample at least twice as fast the highest turbulence frequency to be measured. The algorithm being developed at UTSI takes advantage of the random character of the data acquisition to prevent aliasing and studies show that with a sufficient number of data points the sample rate can be much lower than the highest turbulence frequency to be measured. Because of the apparent periodic character of the flow plotted in Fig 12, the UTSI algorithm was applied to the precursor flow in order to estimate the power spectrum. Figures 27 a-h show the results of the power spectrum computation for 50 Hz intervals and using the velocity time data for the first 6 milliseconds after trigger. As might be expected, a broad range of amplitudes and frequencies is shown. Any detailed consideration of this data and its relation to flow interpretation is beyond the scope of this paper. However, we do find it extremely interesting that a pronounced peak in the power spectrum occurs at a frequency of about 13.5 KHz. If this value is divided into the mean velocity of the flow for the sample interval a length of about 20-mm is found. If this length can be interpreted as proportional to some turbulence scale length, then an apparently reasonable correlation has been found with barrel diameter.

4.0 SUMMARY AND CONCLUSIONS

A dual scatter laser velocimeter has been shown to be capable of obtaining velocity measurements in muzzle blasts from a 20-mm cannon. Data have been obtained at selected positions on the projectile trajectory and near its edge. Velocity values ranging from subsonic to supersonic were detected. Data rate acquisition capability was limited to about 22 milliseconds. This sampling rate was limited by the data transfer characteristics of the computer memory used to store the velocity processor measurements and the time at which the measurements were made. In order to accurately characterize the velocity structure of the flow much higher sampling rates are required—probably of the order of 10^3/millisecond. Such sampling rate capability is within current state-of-the-art, but would require careful

interrogation of a high speed LV signal processor with a large microprocessor memory.

In examining these data it should be borne in mind that only one velocity component was measured (that parallel to the centerline) and that the sign of the velocity vector was not determined. Future measurements involving a directionally sensitive LV and perhaps measuring two velocity components would probably yield data of much greater value than that presented here.

A new algorithm under development at UTSI was used to estimate the power spectral density of the precursor flow at X/D = 3, Y/D = 0. The results yield a turbulence scale of the order of the muzzle diameter.

Transmission measurements made through the flow using one of the transmitted LV beams proved to be a useful technique for determining when the projectile passed the probe volume and when strong flow field fluctuations occurred.

We conclude that the laser velocimeter is an acceptable means for obtaining velocity measurements in muzzle blasts. Data quality should be greatly improved by increasing the data sampling rate and by using a directionally sensitive two component instrument.

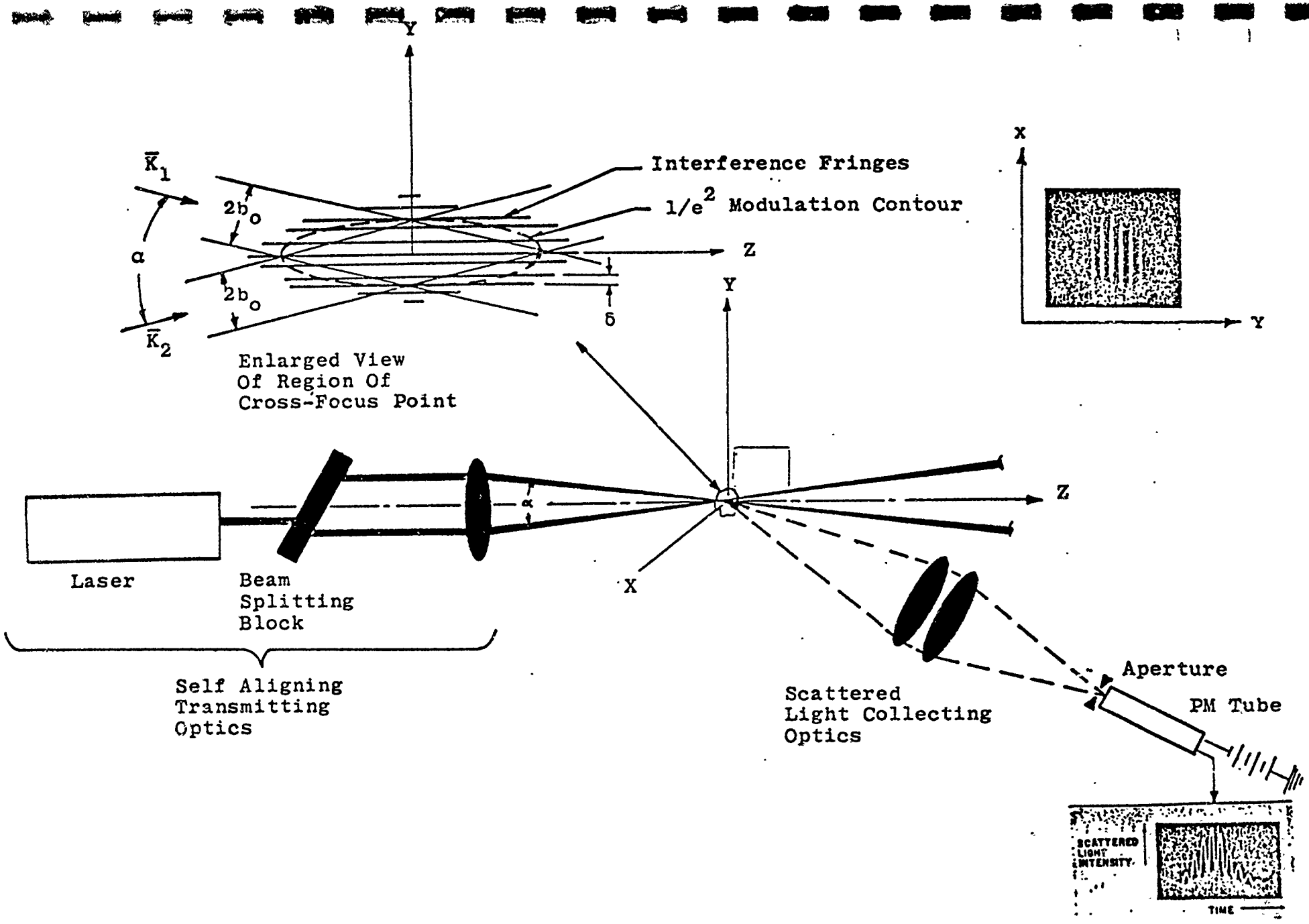

Figure 1. Typical optical arrangement for generating and observing a set of well-defined interference fringes.

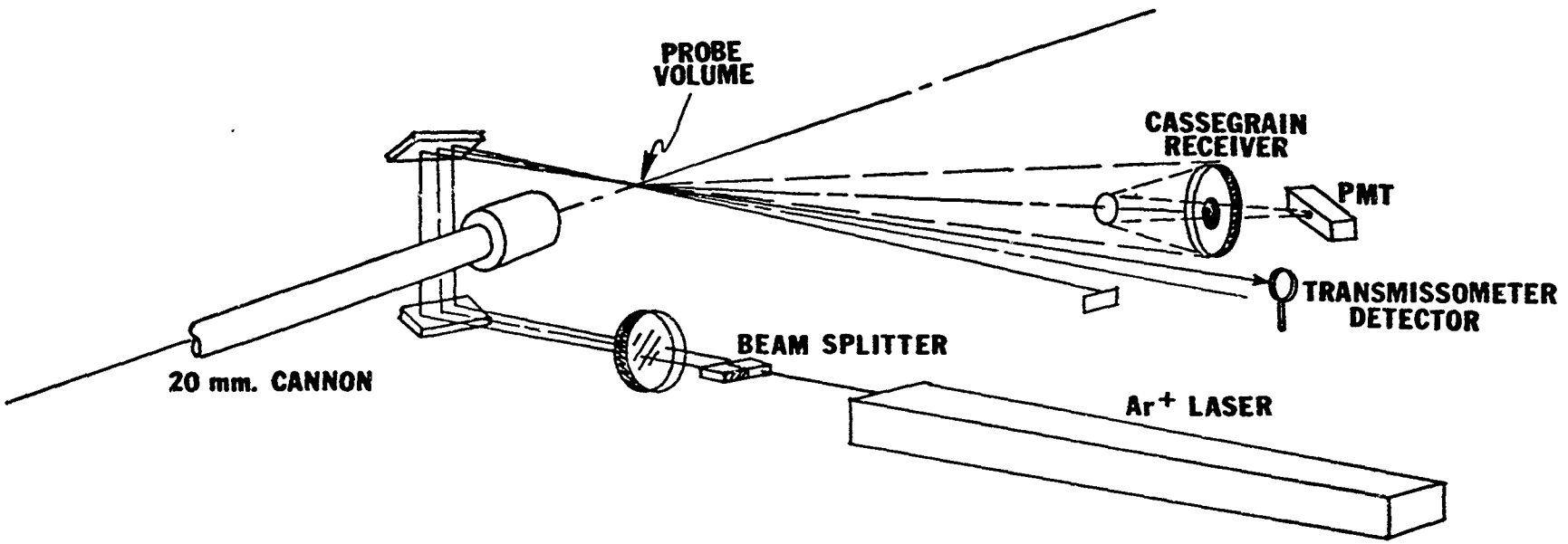

Figure 2. LV optical system arrangement for muzzle blast measurements.

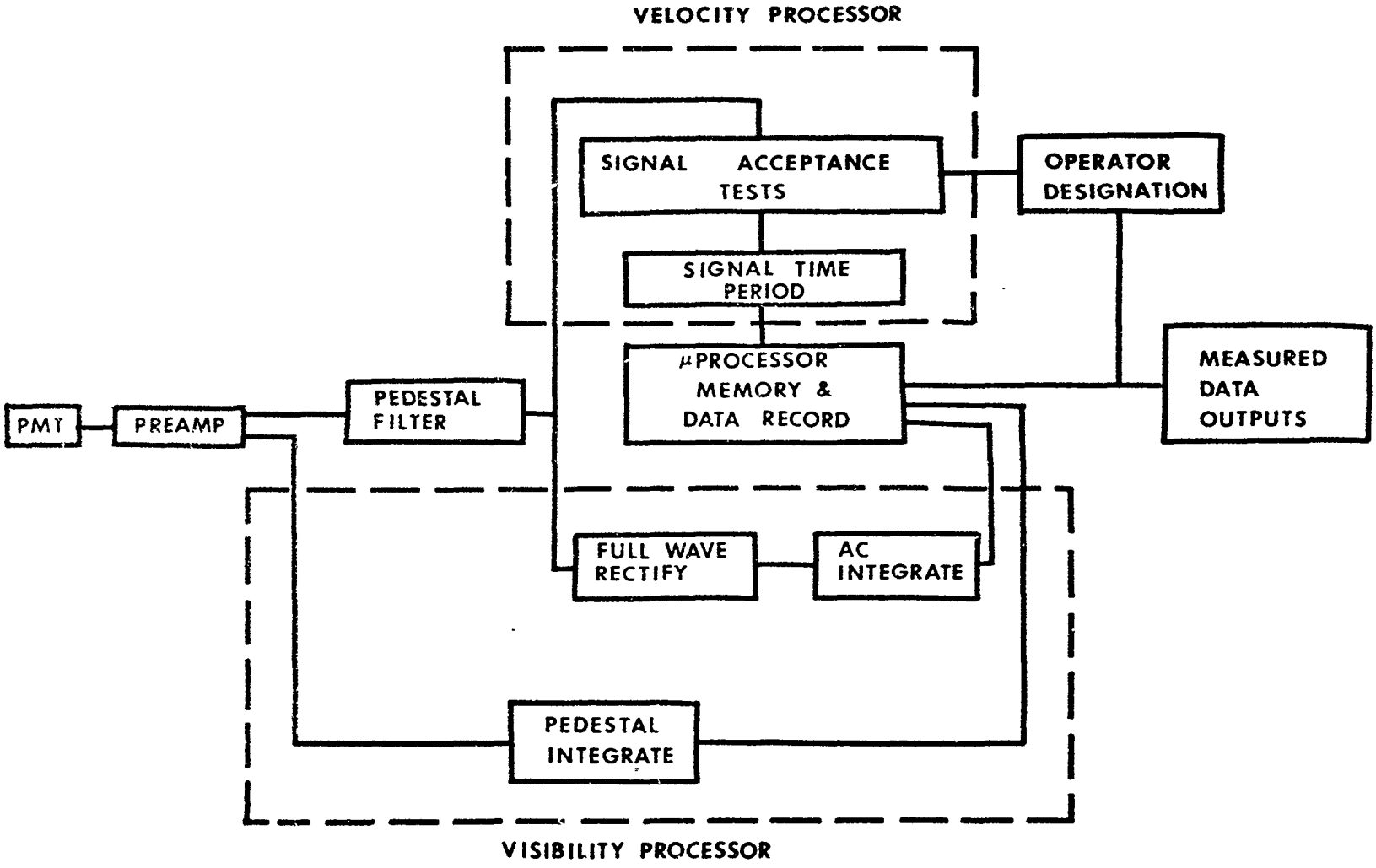

Figure 3. Schematic of Signal Processing System.

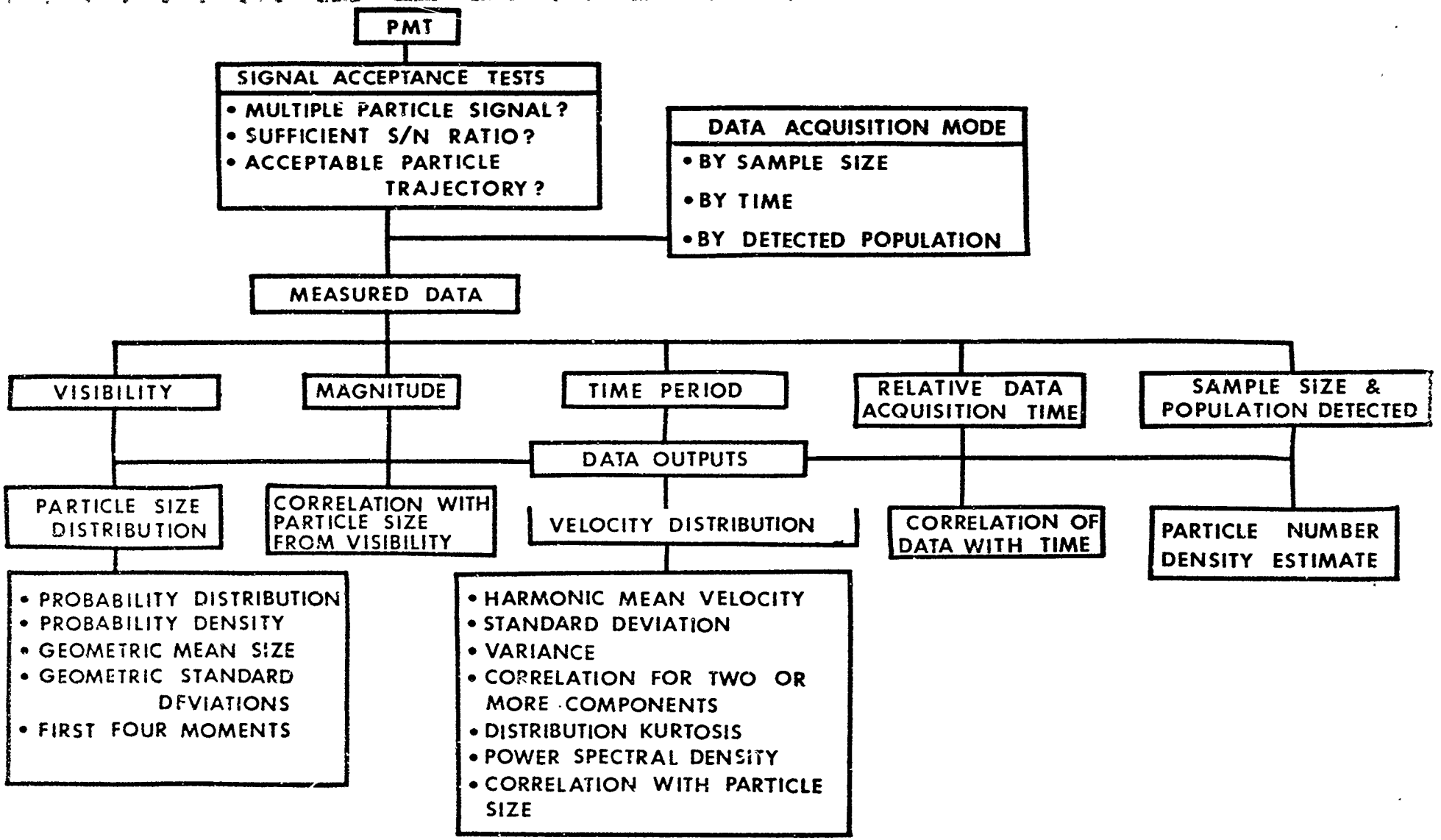

PSI MEASUREMENT FUNCTIONS AND DATA OUTPUTS

Figure 4. Schematic of Data Acquistion Measurement Functions.

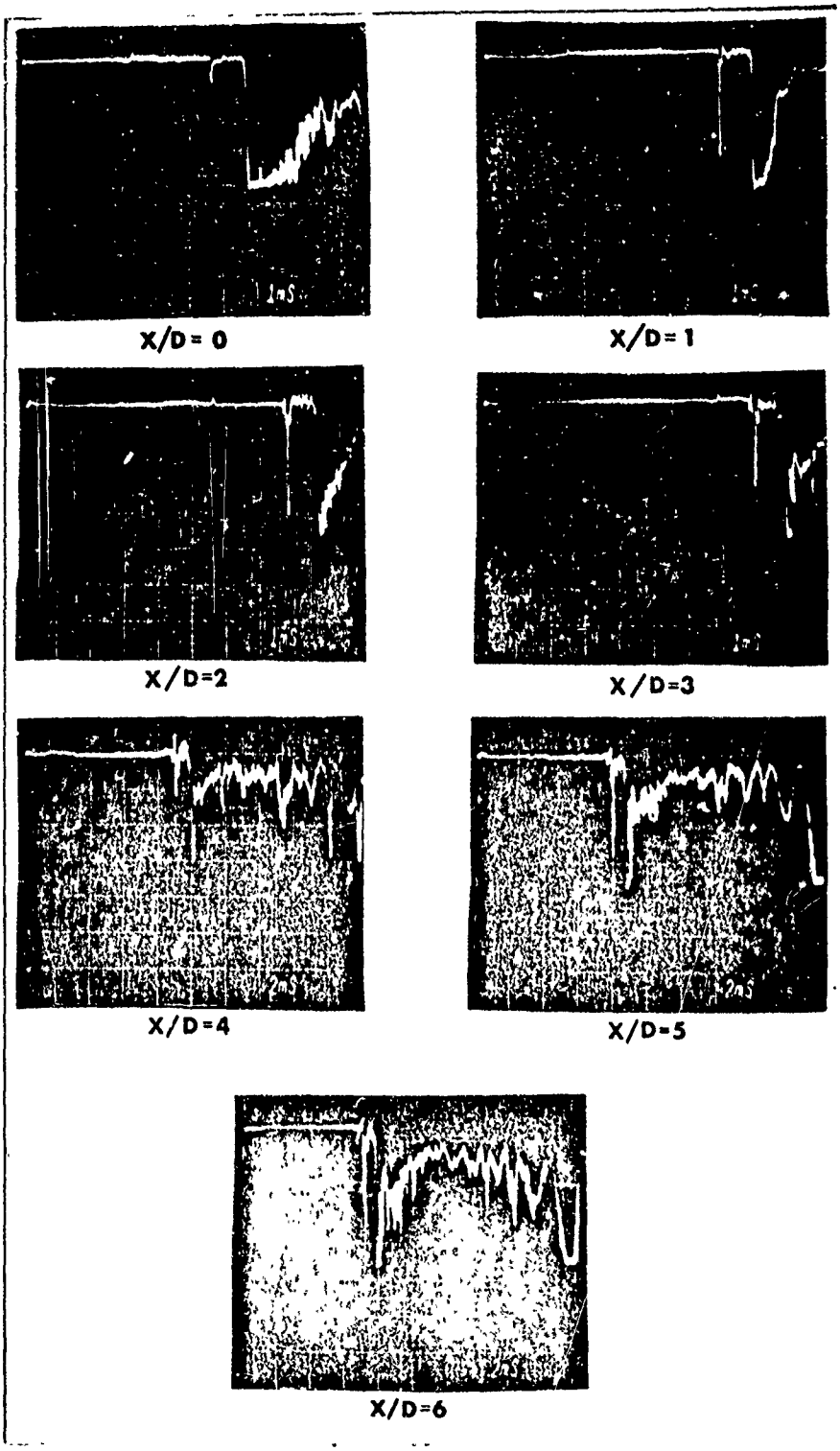

Figure 5. Transmissometer outputs for measurements along Y/D = 0.

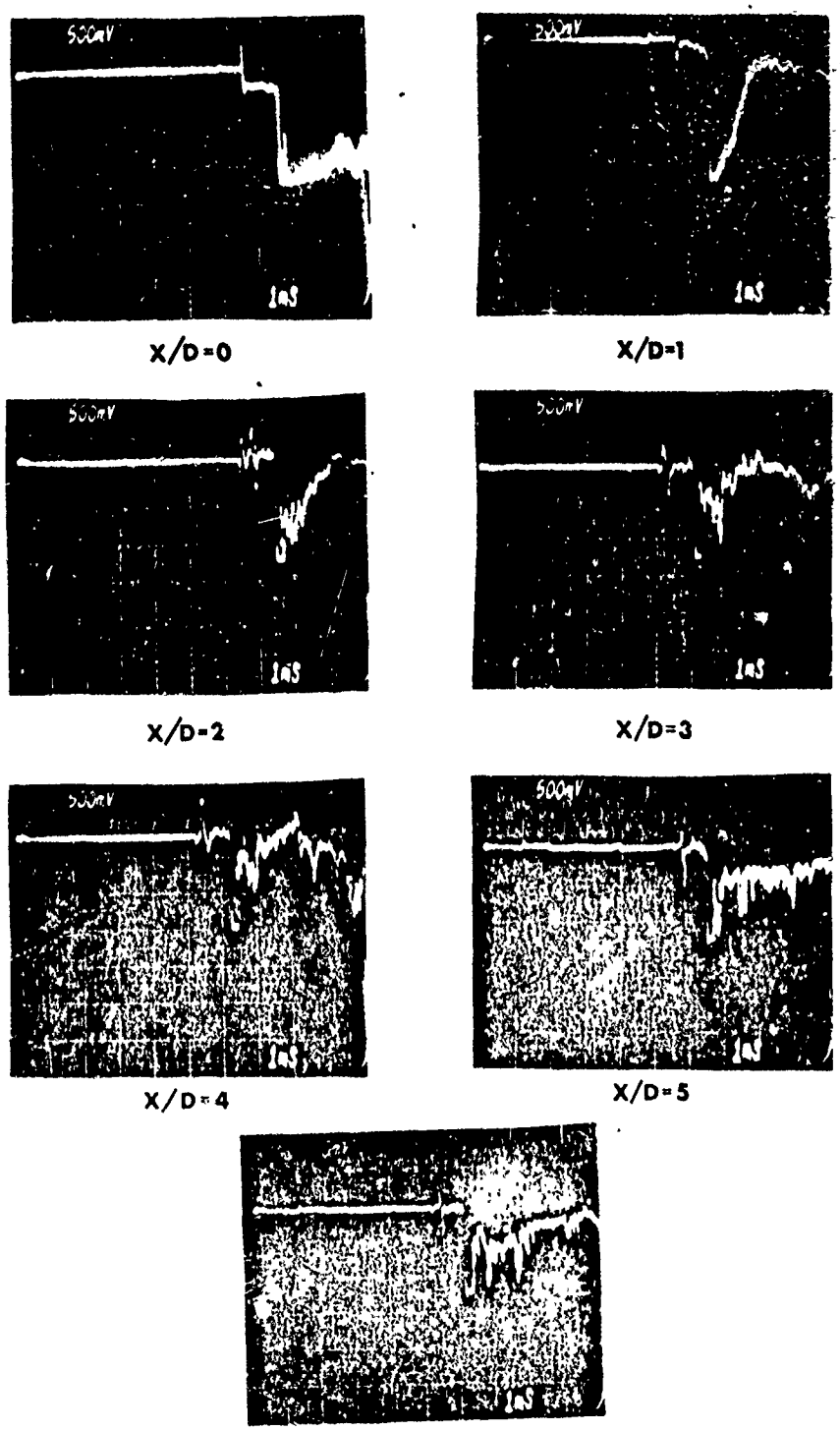

Figure 6. Transmissometer outputs for measurements along Y/D = -0.5.

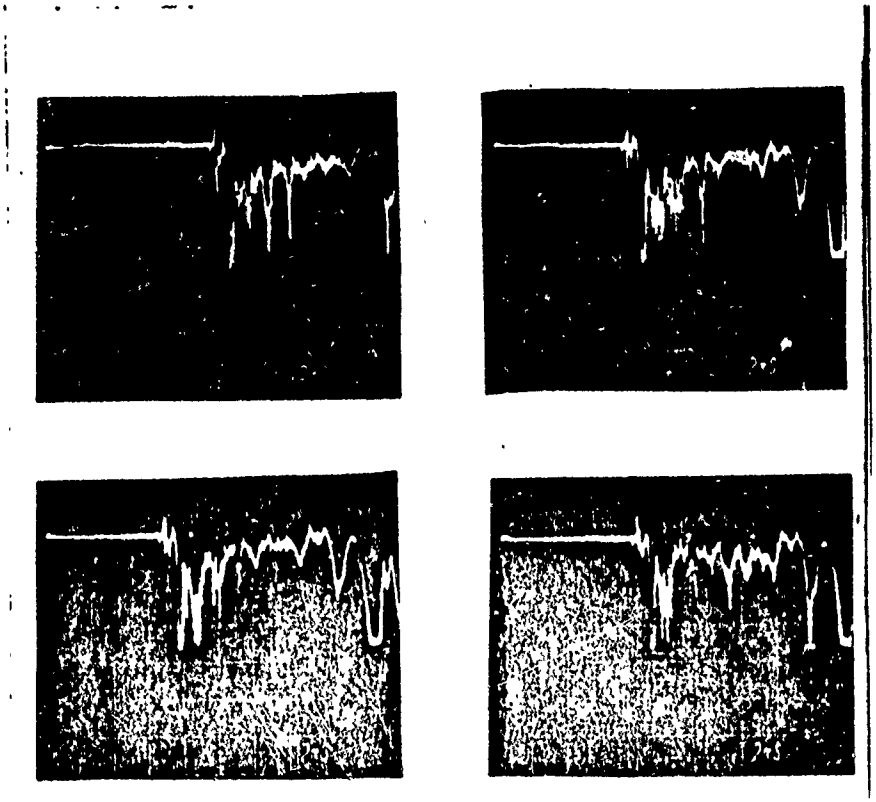

Figure 7. Transmissometer outputs for 4 consecutive shots at Y/D = -0.5, X/D = 7.0.

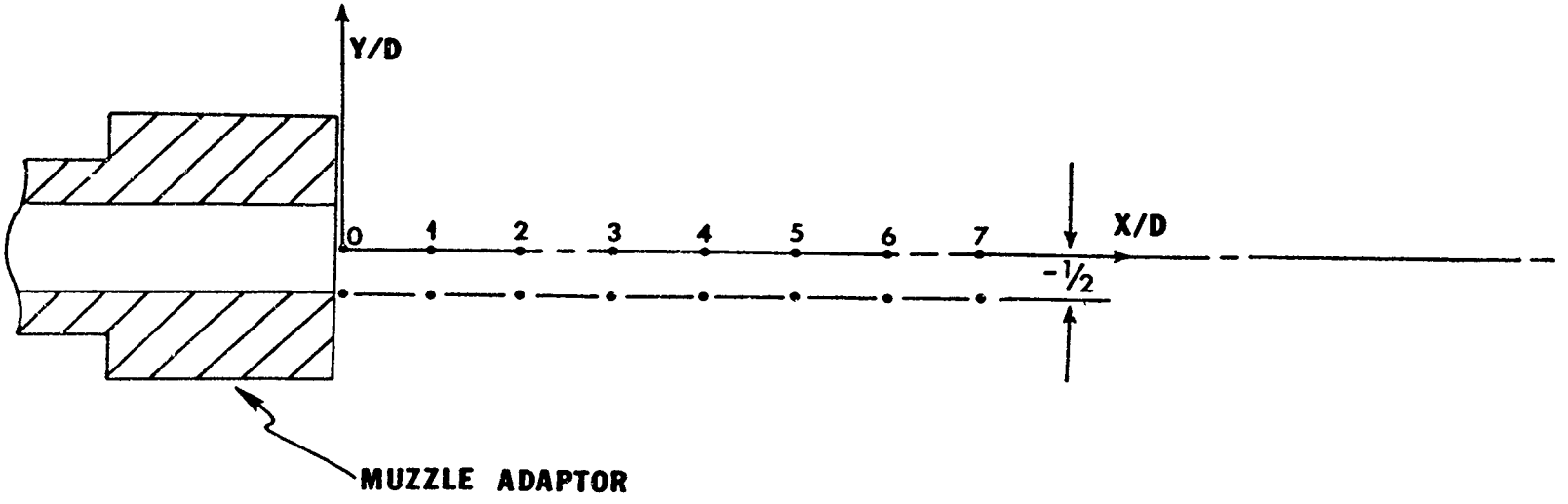

Figure 8. Location of data measurement stations..

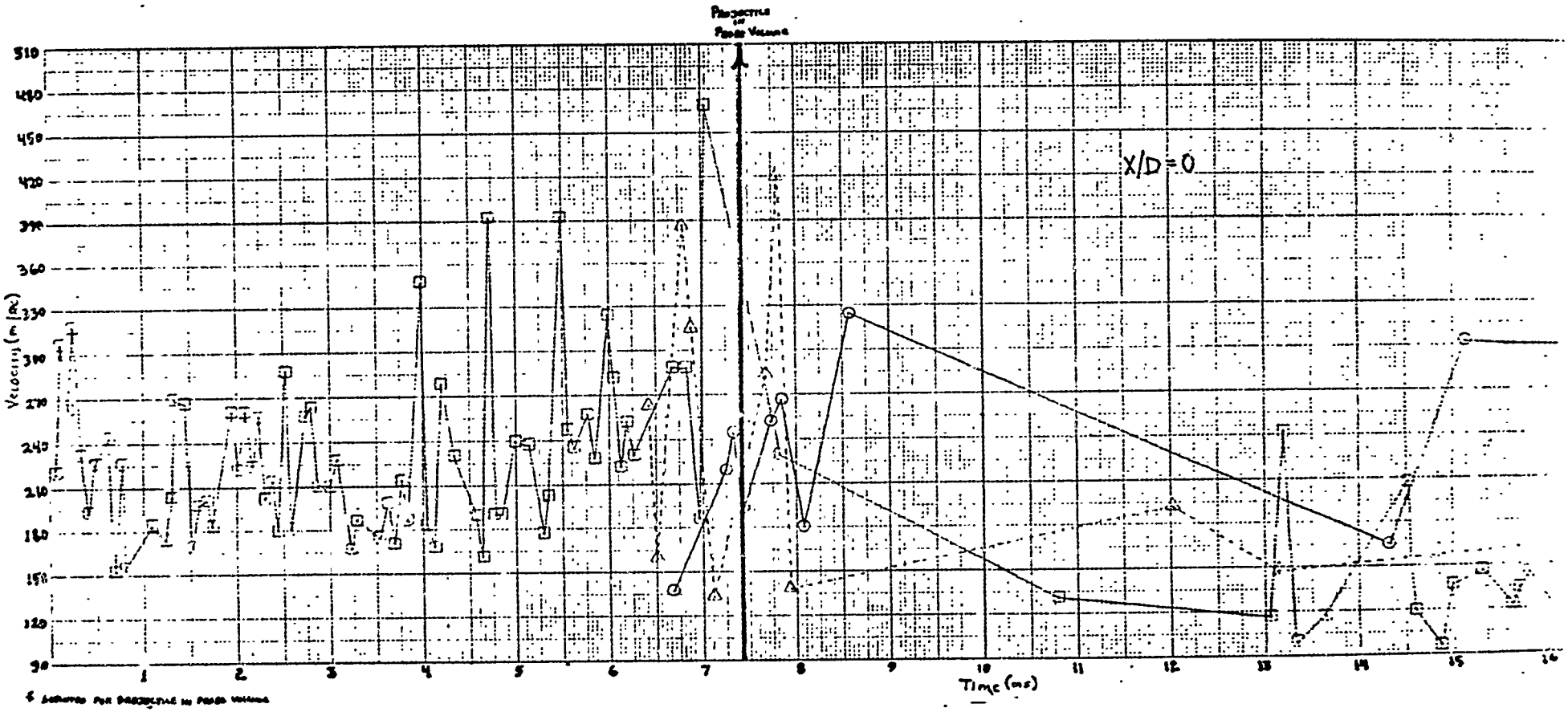

Figure 9. Velocity versus Time for Y/D = 0, X/D = 0.

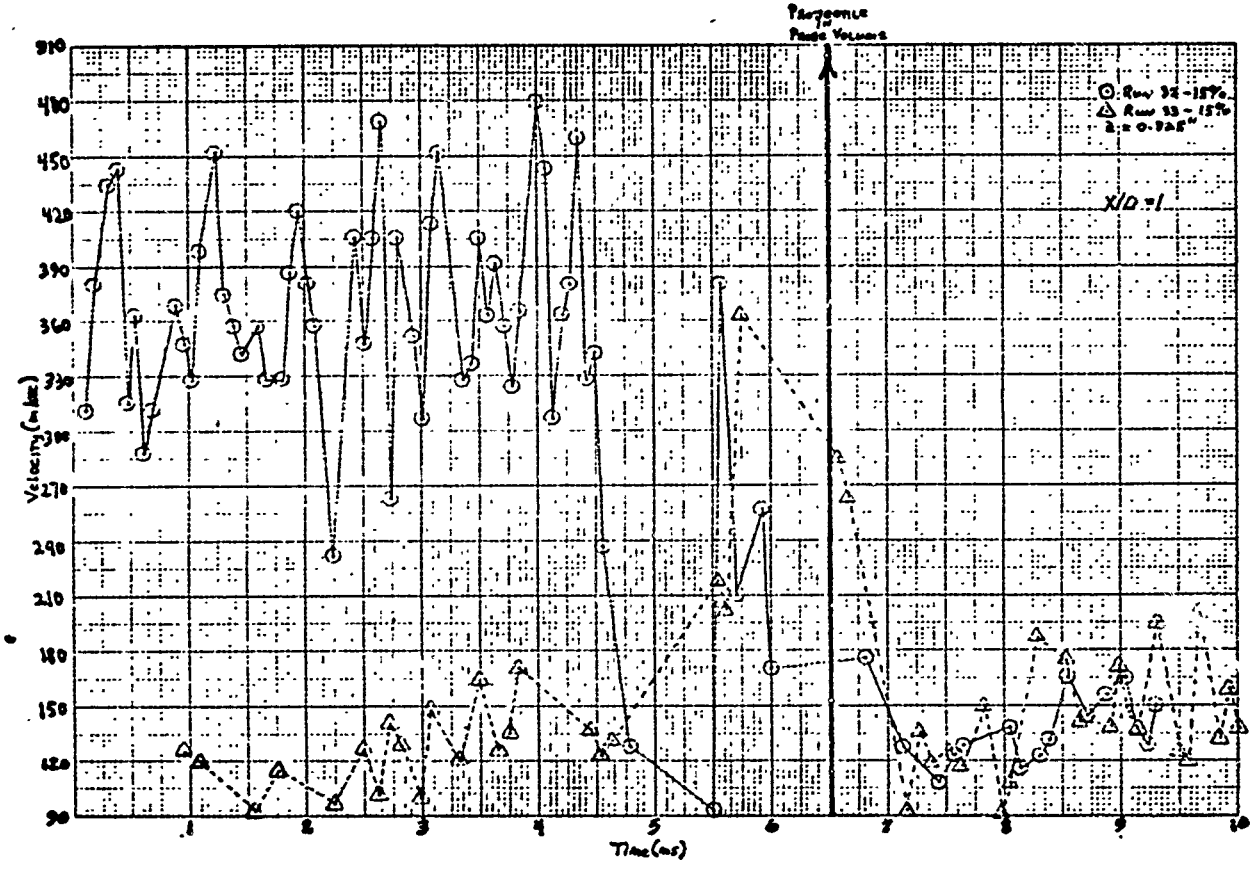

Figure 10. Velocity versus Time for Y/D = 0, X/D = 1.

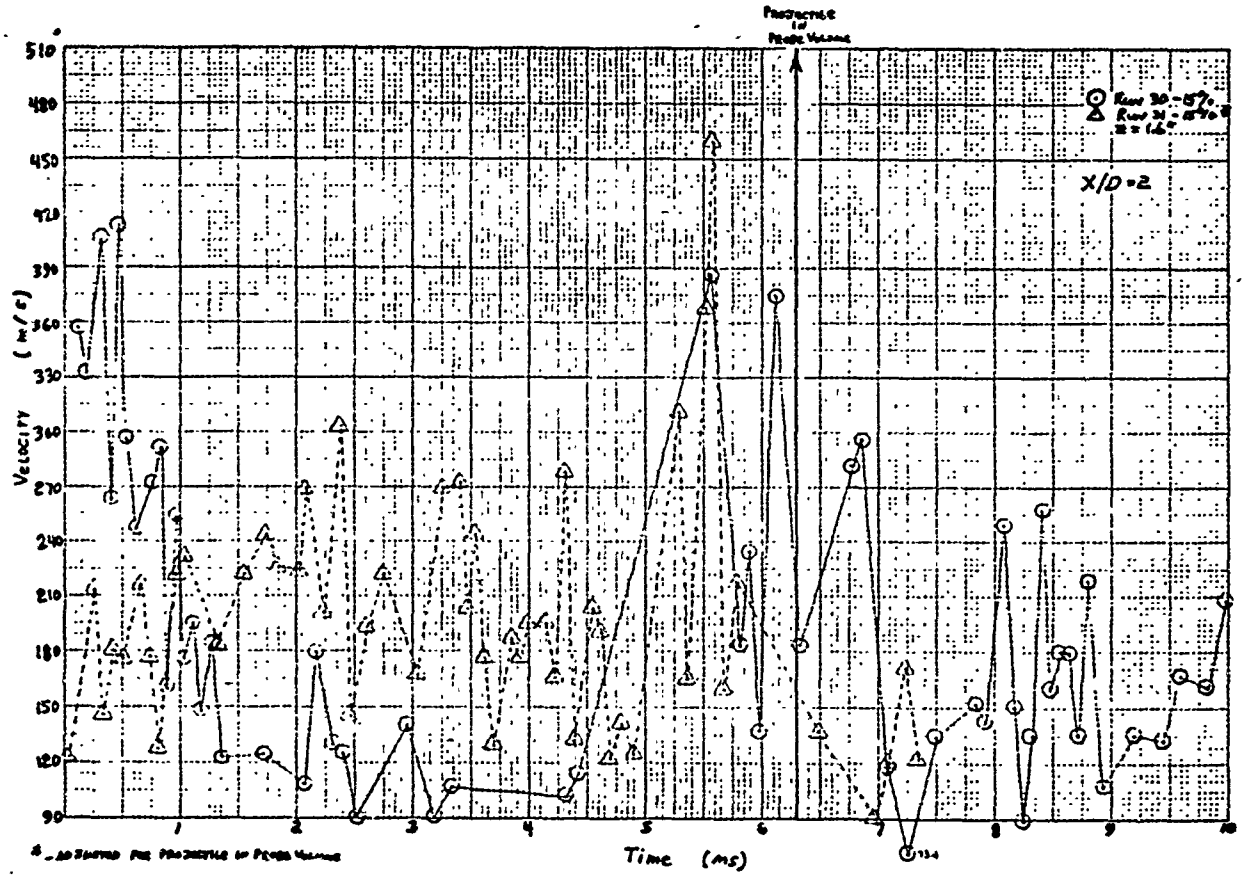

Figure 11. Velocity versus Time for Y/D = 0, X/D = 2.

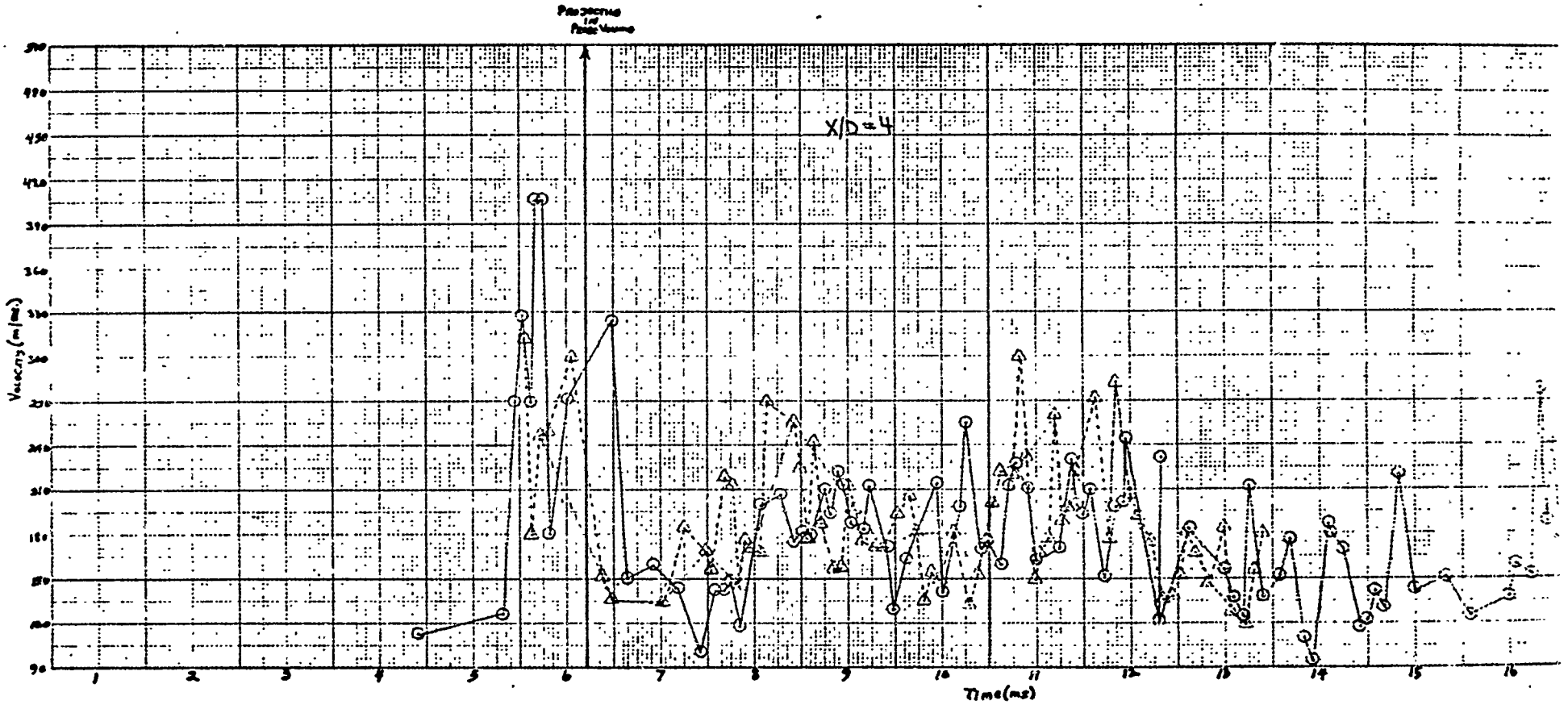

Figure 13. Velocity versus Time for Y/D = 0, X/D = 4.

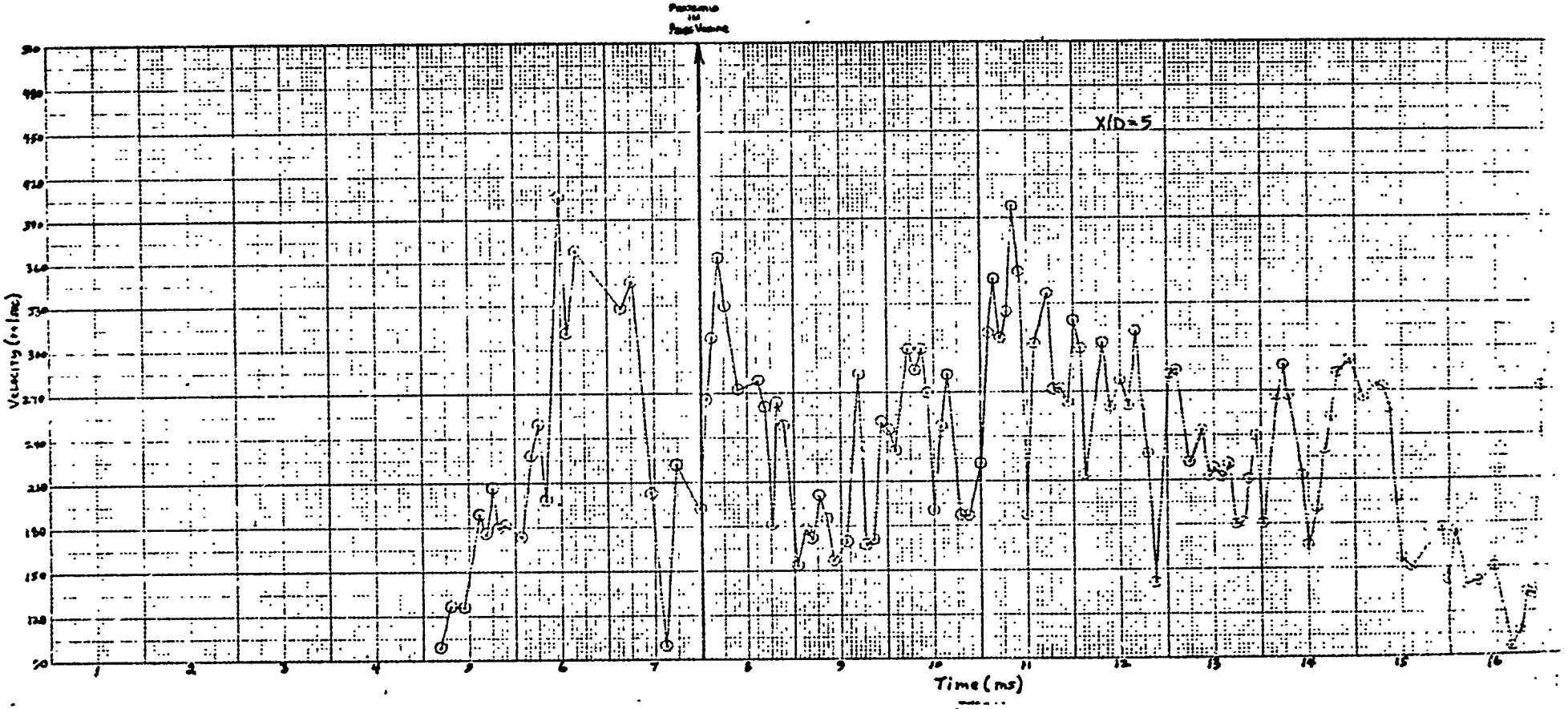

Figure 14. Velocity versus Time for Y/D = 0, X/D = 5.

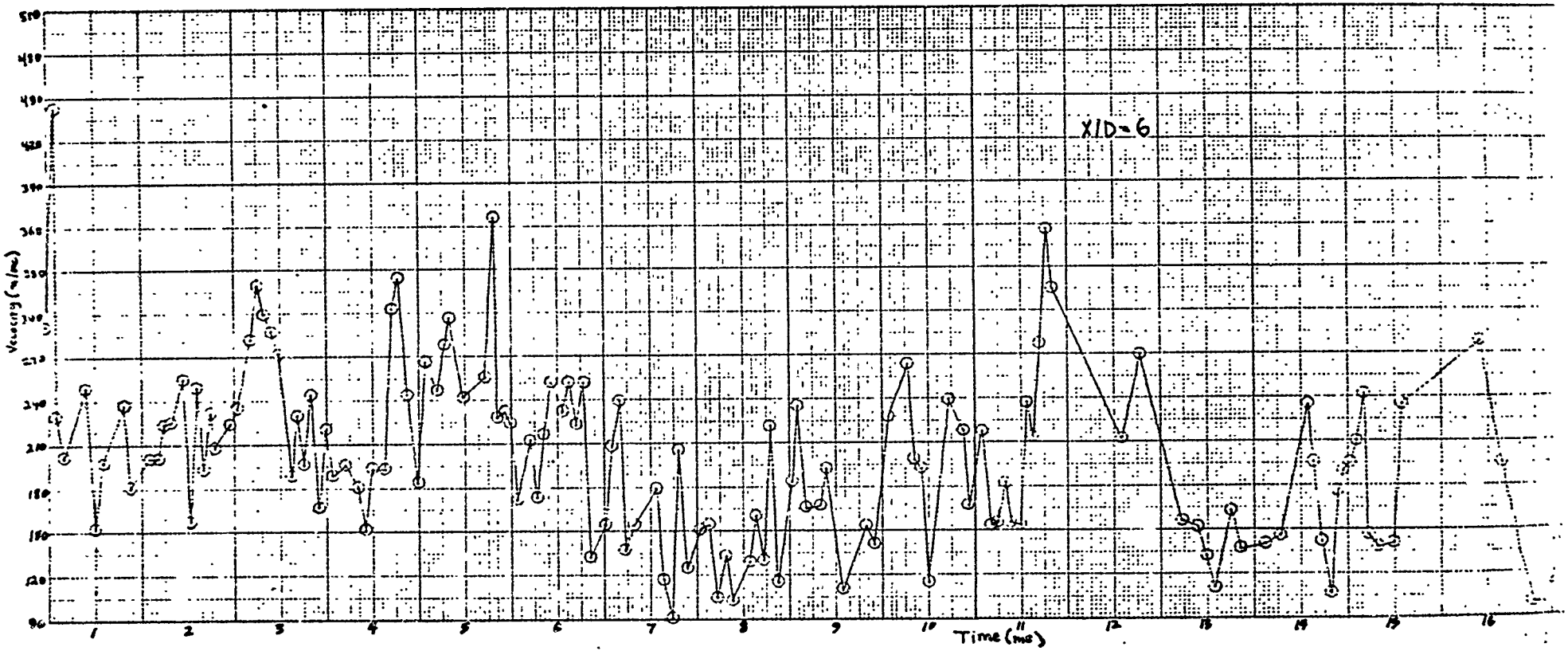

Figure 15. Velocity versus Time for Y/D = 0, X/D = 6.

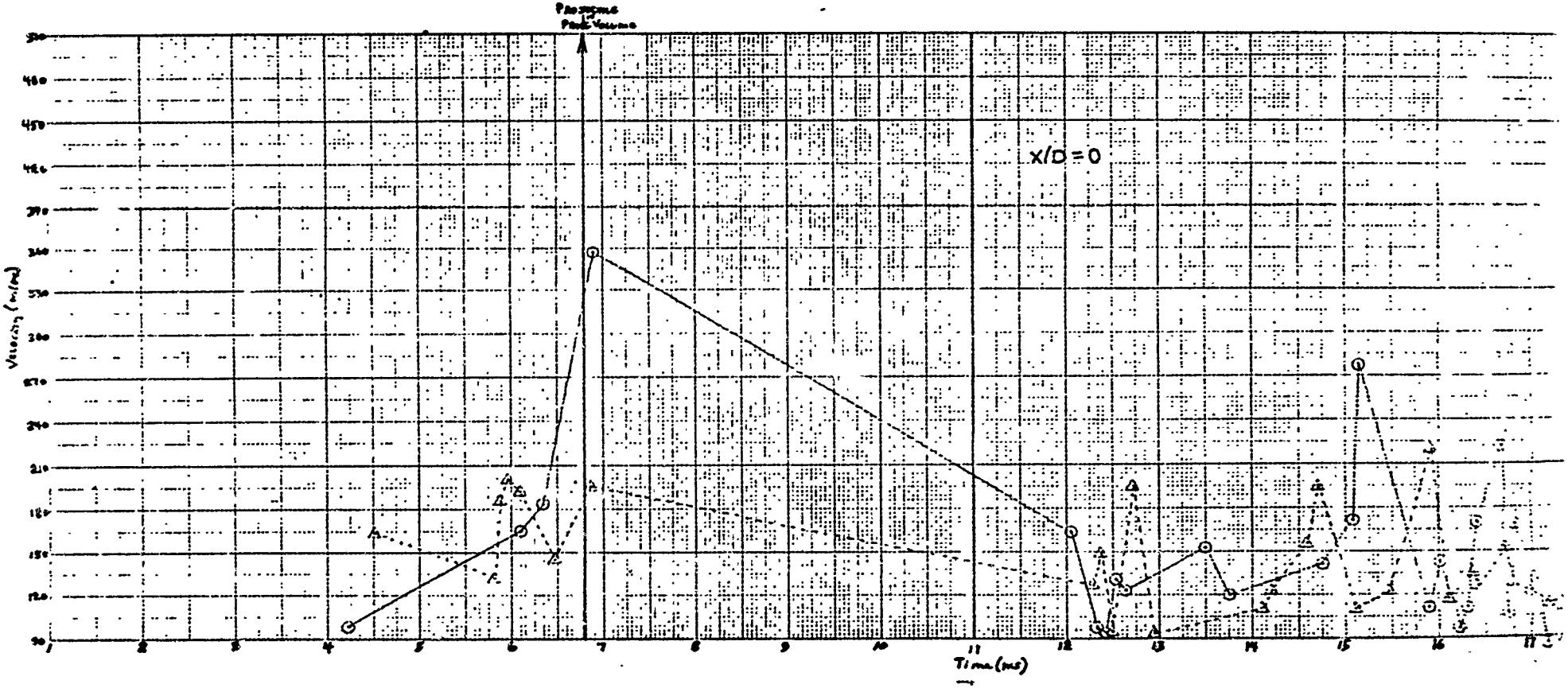

Figure 16. Velocity versus Time for Y/D = -0.5, X/D = 0.

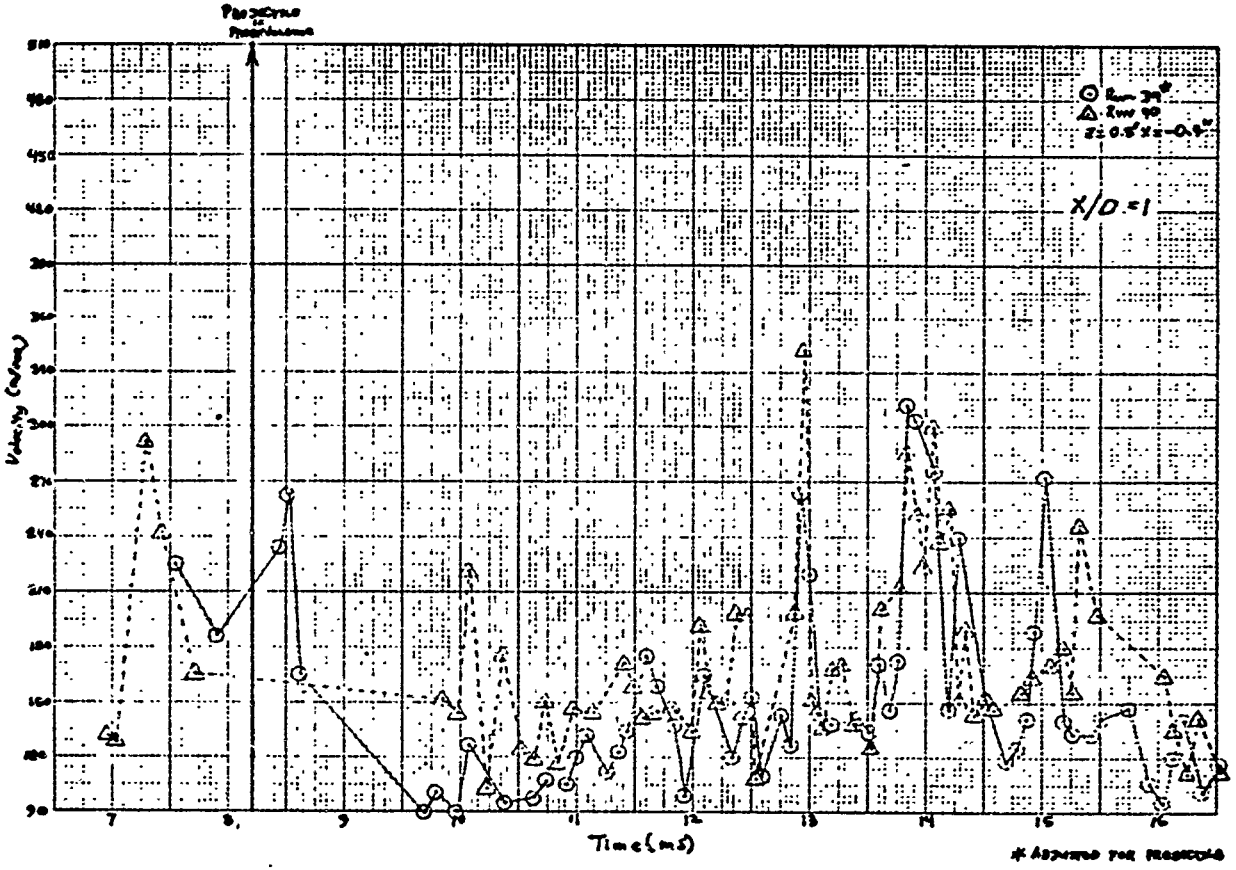

Figure 17. Velocity versus Time for Y/D = -0.5, X/D = 1.

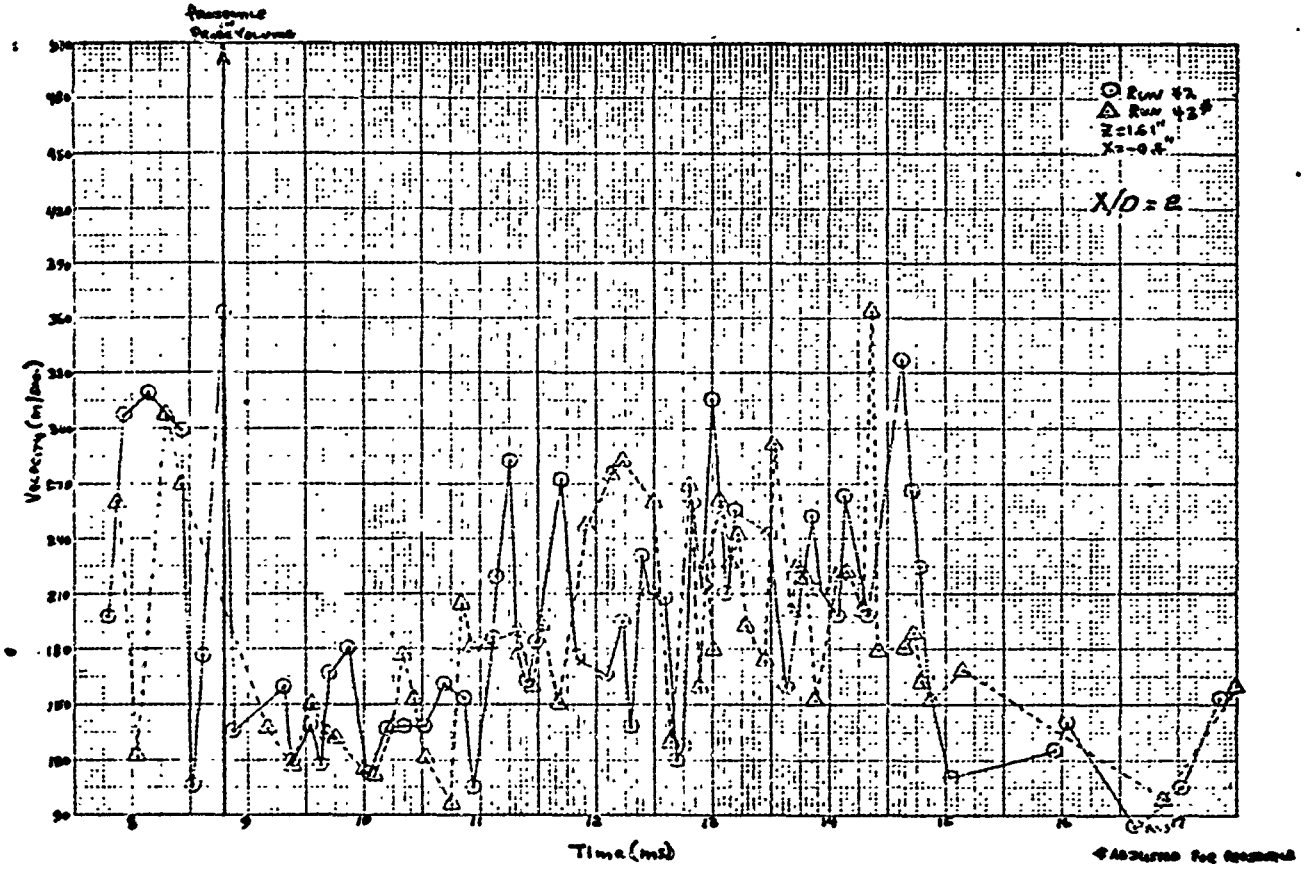

Figure 18. Velocity versus Time for Y/D = -0.5, X/D = 2.

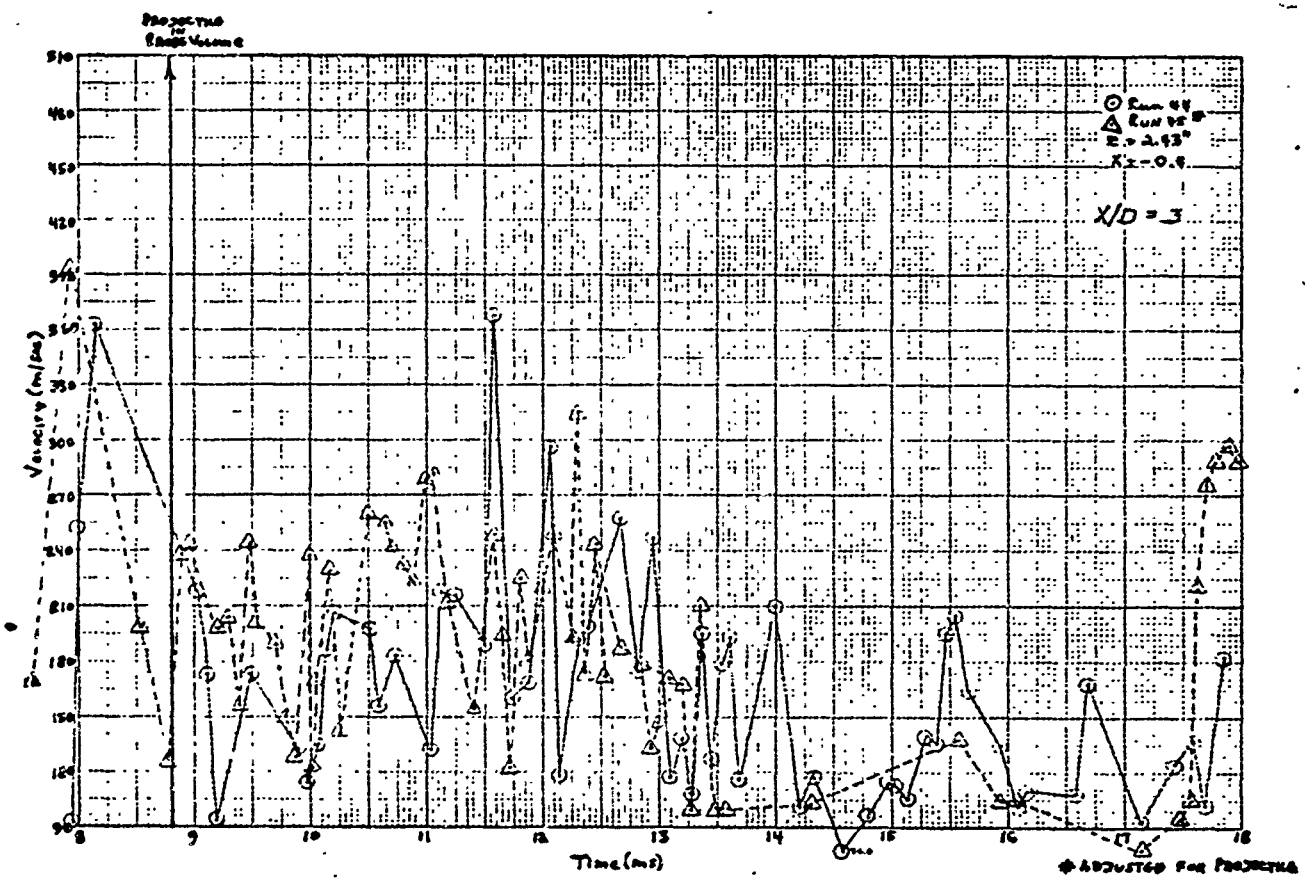

Figure 19. Velocity versus Time for Y/D = -0.5, X/D = 3.

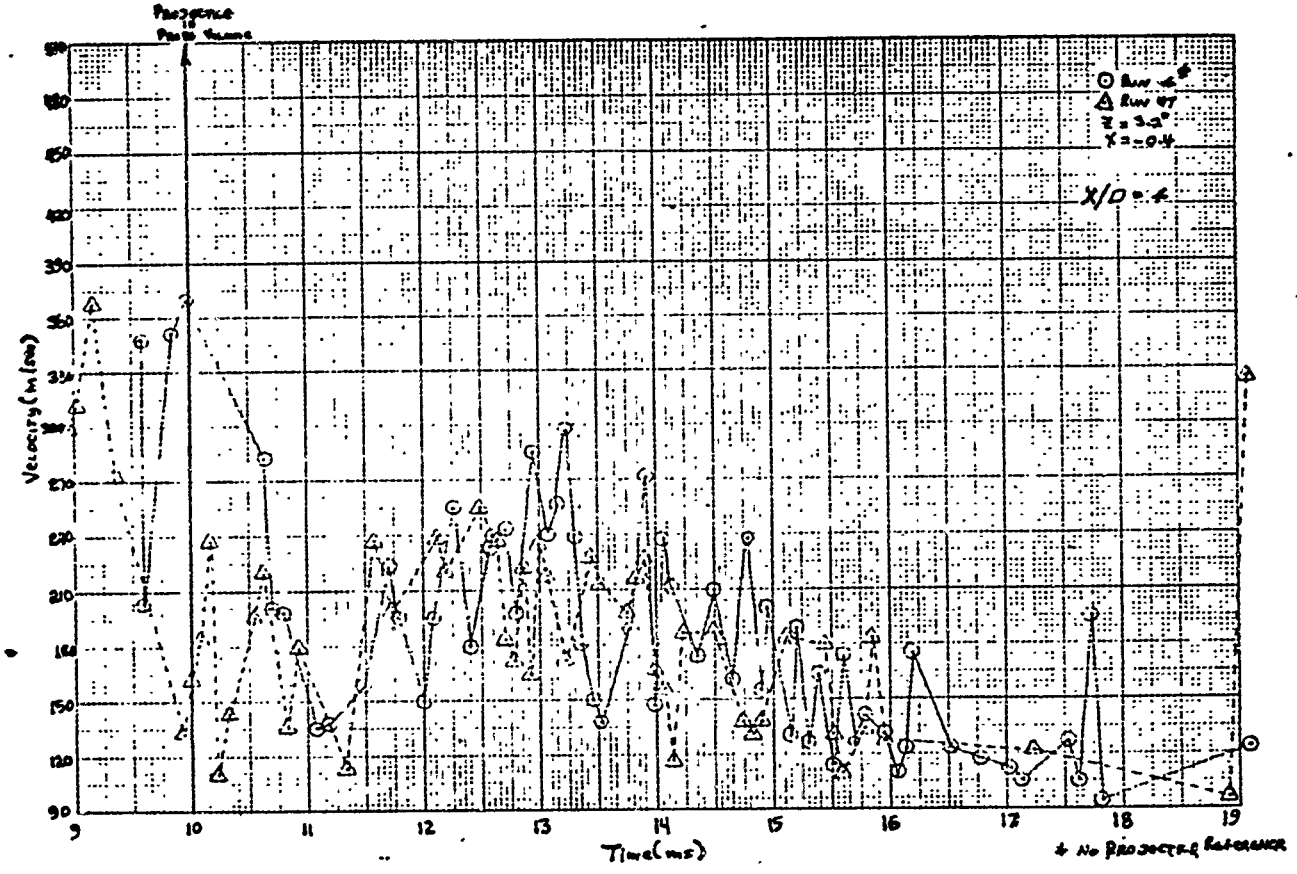

Figure 20. Velocity versus Time for Y/D = -0.5, X/D = 4.

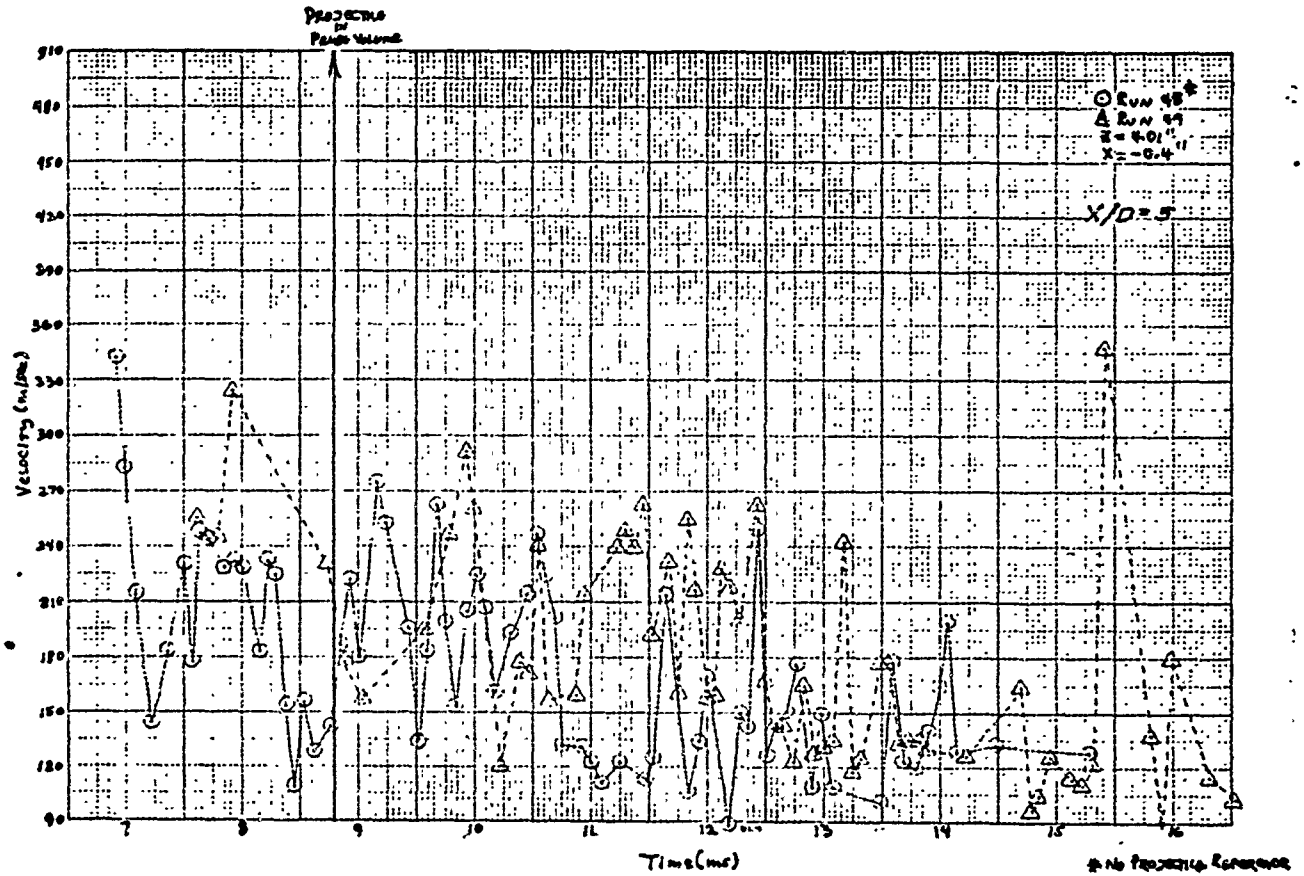

Figure 21. Velocity versus Time for Y/D = -0.5, X/D = 5.

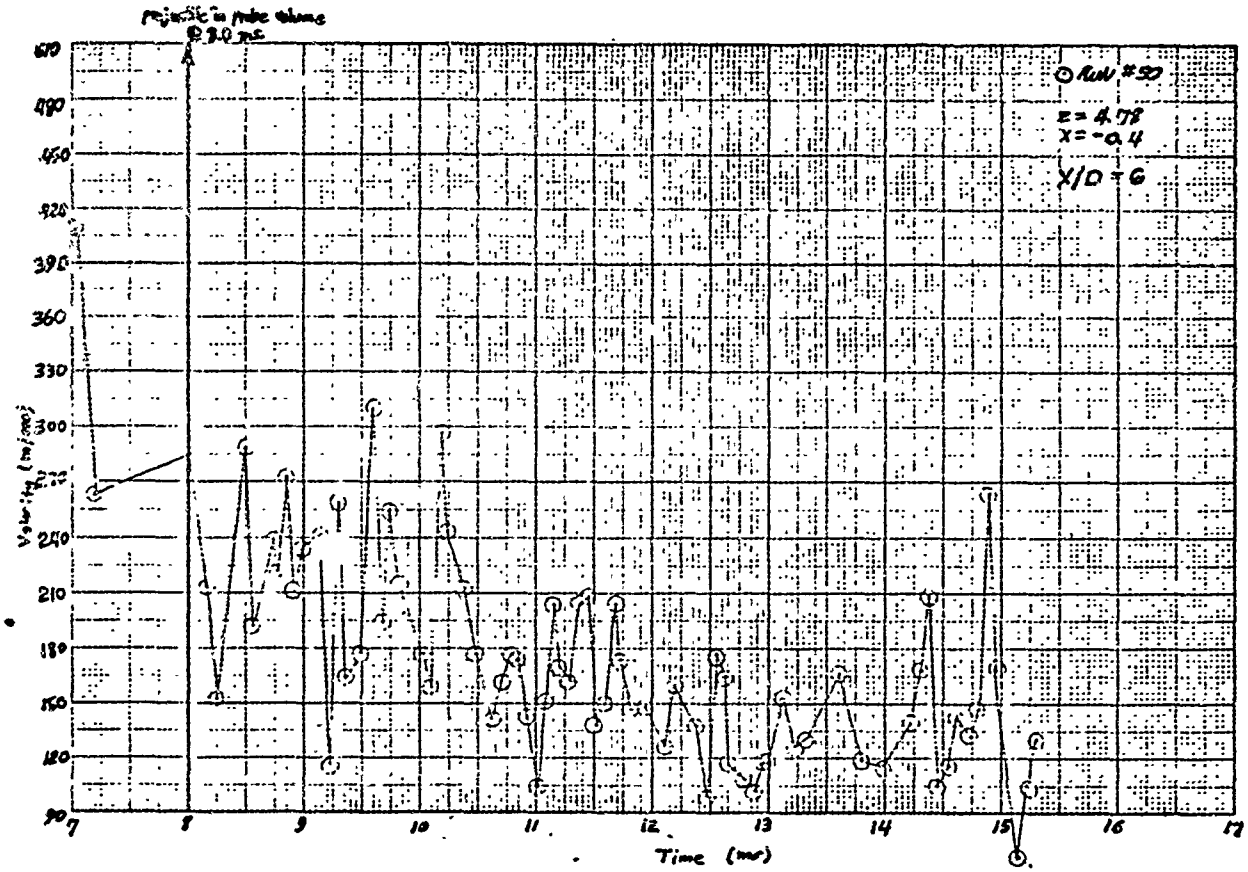

Figure 22. Velocity versus Time for Y/D = -0.5, X/D = 6.

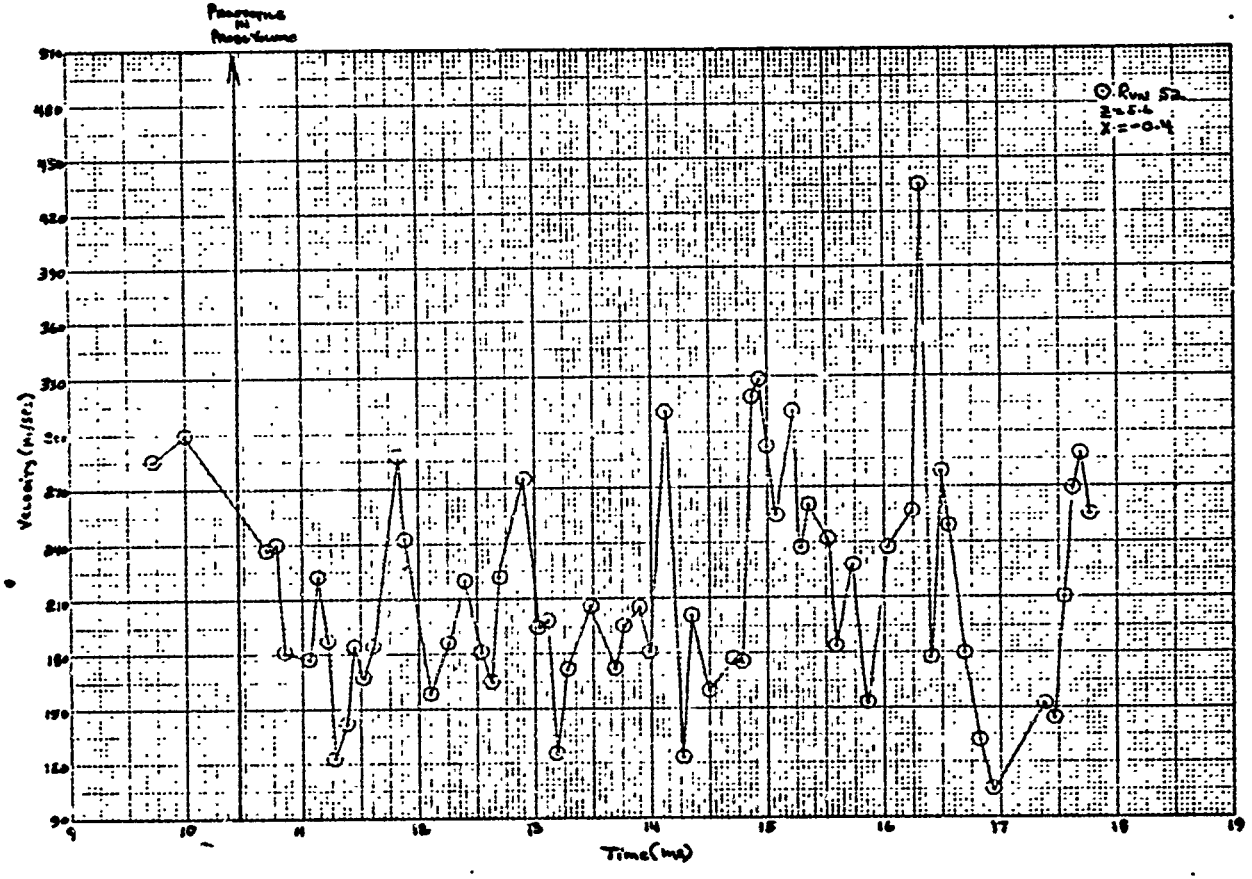

Figure 23. Velocity versus Time for 4 consecutive firings at Y/D = -0.5, X/D = 7.0 : Shot 1.

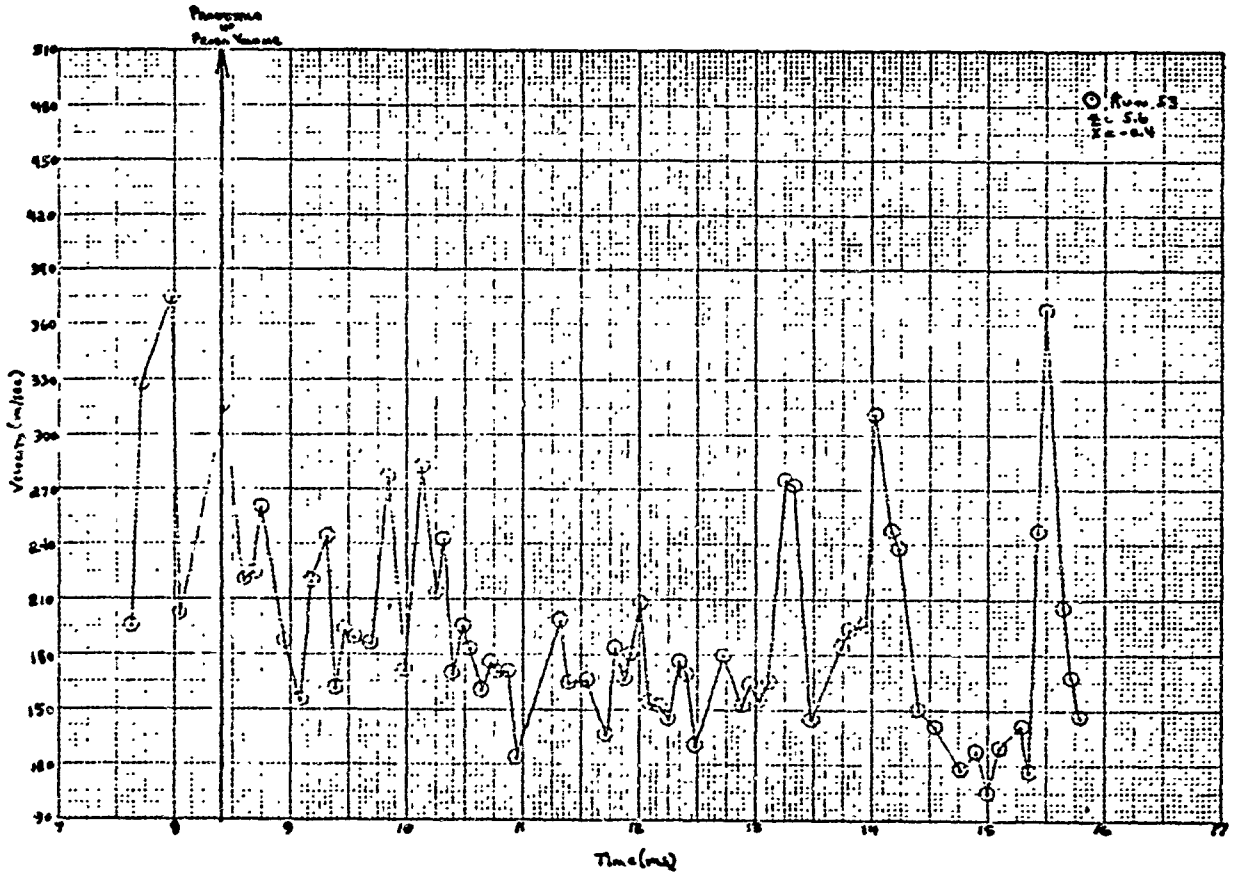

Figure 24. Velocity versus Time for 4 consecutive firings at Y/D = -0.5, X/D = 7.0 : Shot 2.

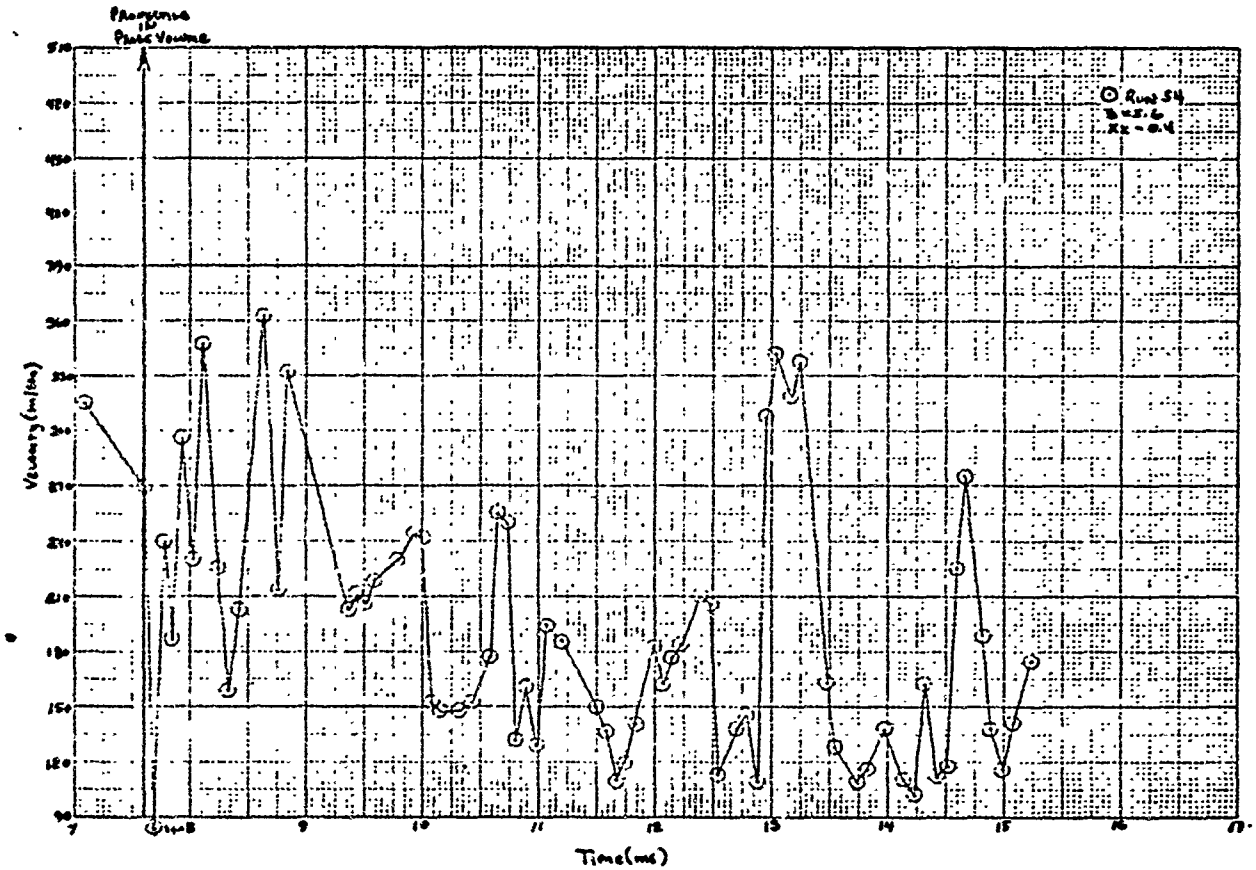

Figure 25. Velocity versus Time for 4 consecutive firings at Y/D = -0.5, X/D = 7.0 : Shot 3.

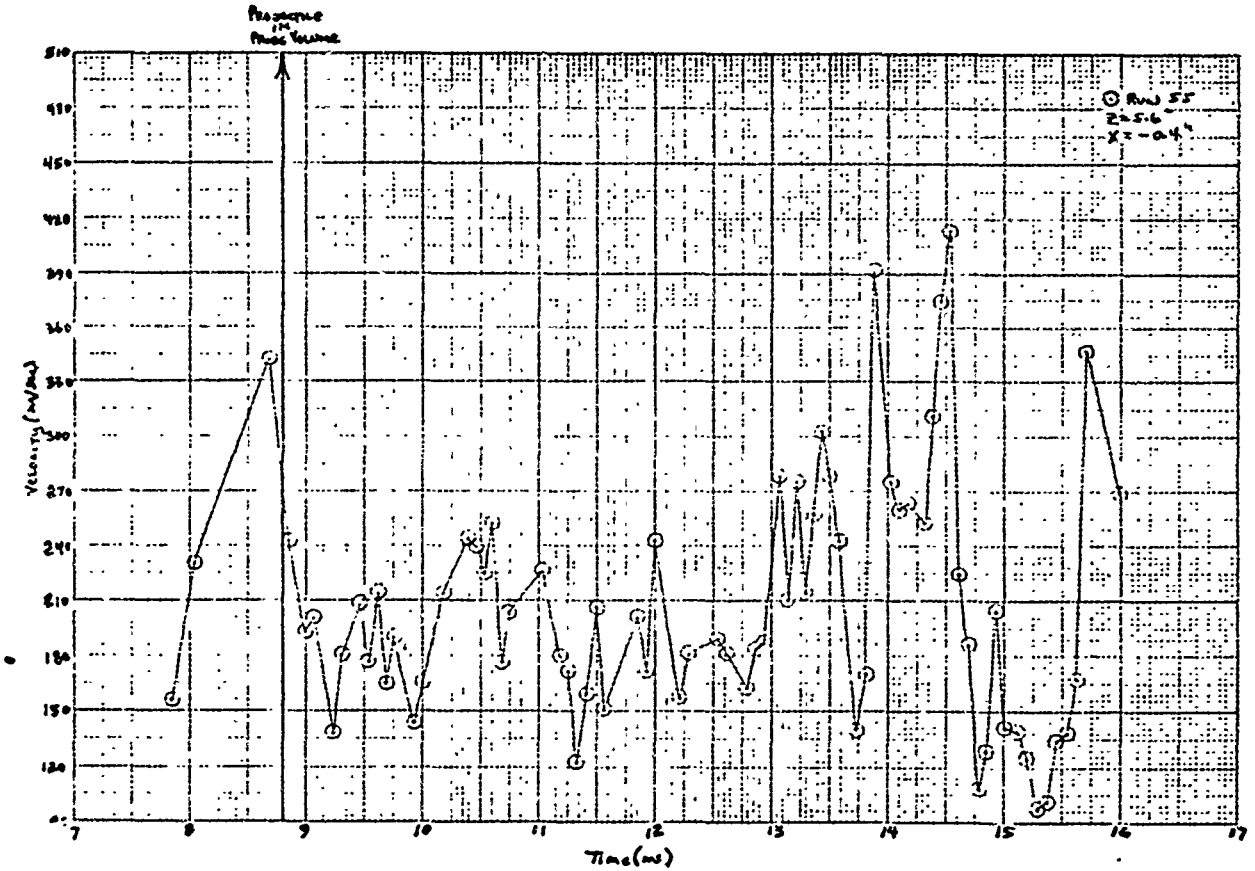

Figure 26. Velocity versus Time for 4 consecutive firings at Y/D = -0.5, X/D = 7.0 : Shot 4.

Figure 27a. Power Spectral Density for Y/D = 0, X/D = 3, 50 - 2750 Hz.

Figure 27b. Power Spectral Density for Y/D = 0, X/D = 3, 2800 - 5550 Hz.

Figure 27c, Power Spectral Density for Y/D = 0, X/D = 3, 5600 - 8450 Hz.

Figure 27d. Power Spectral Density for Y/D = 0,X/D = 3, 8500 - 11500 Hz.

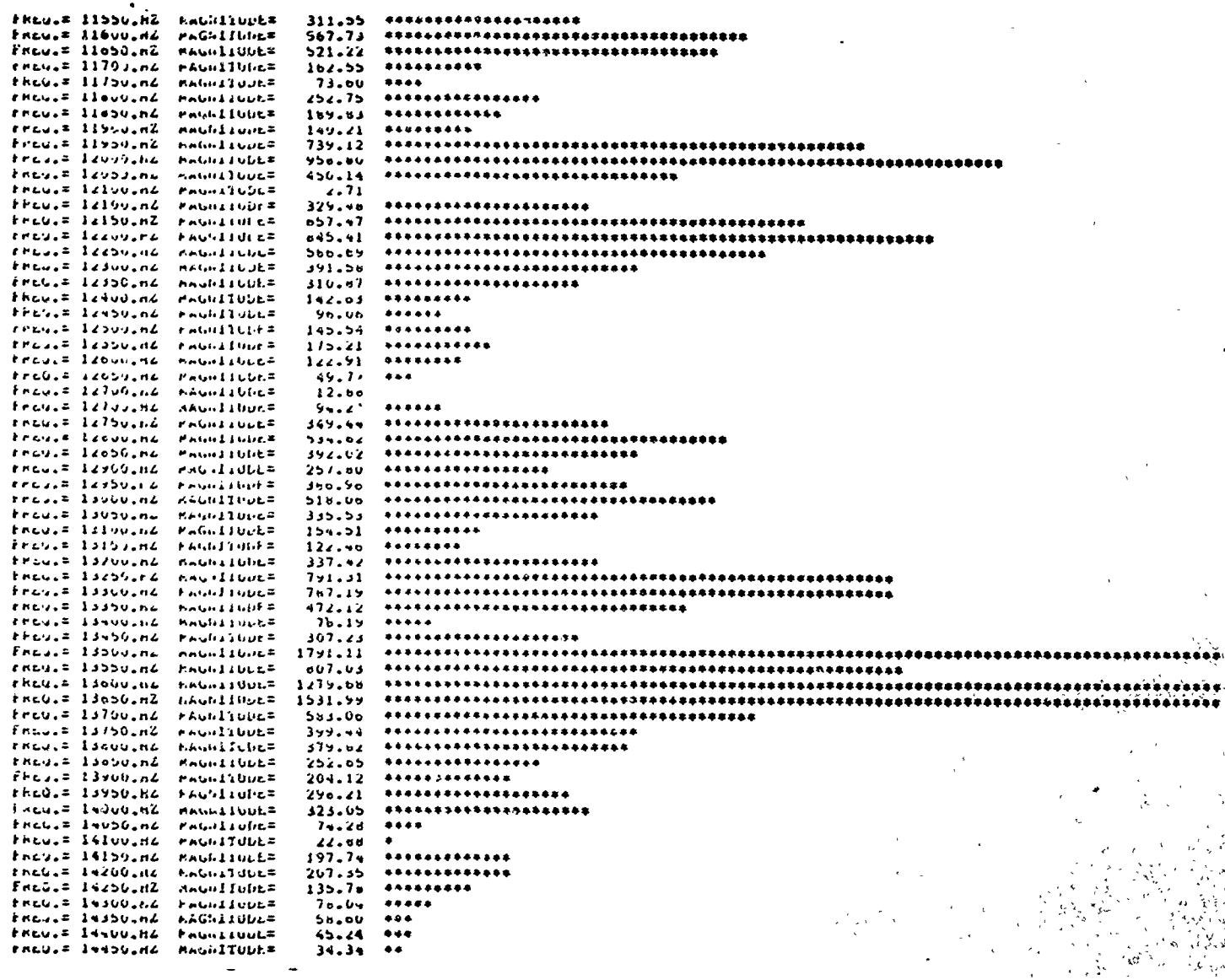

Figure 27e. Power Spectral Density for Y/D = 0, X/D = 3, 11550 - 14450 Hz.

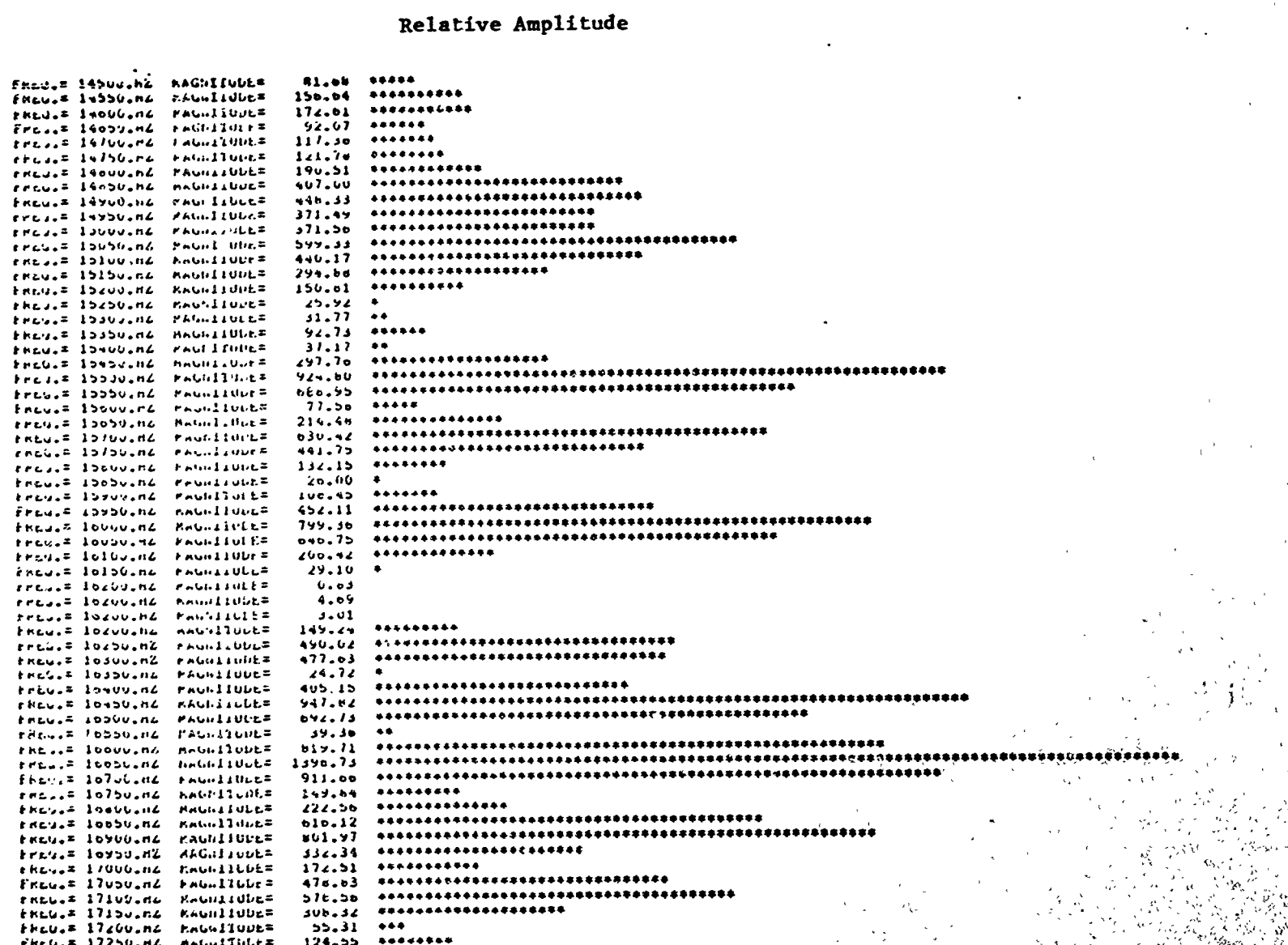

Figure 27f. Power Spectral Density for Y/D = 0, X/D = 3, 14500 - 17350 Hz.

Relative Amplitude

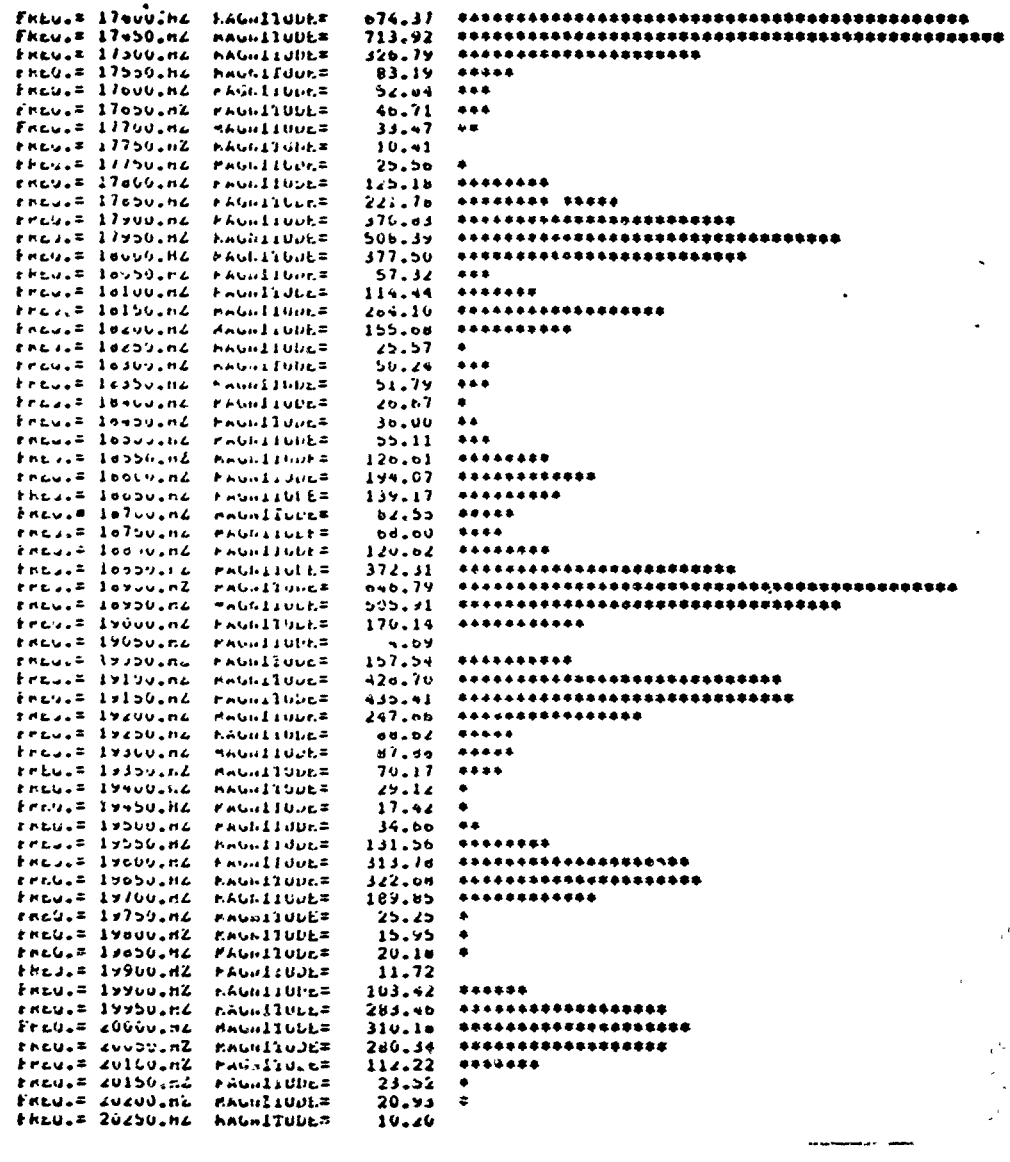

Frequency

Figure 27g. Power spectral Density for Y/D = 0, X/D = 3, 17400 - 20250 Hz.

Figure 27h. Power Spectral Density for Y/D = 0, X/D = 3, 20300 - 23050 Hz.